ANNUAL LETTER REPORT
1988

I. CONTRACT INFORMATION

A. Title: "Far- and Mid-Infrared Properties of Metal-Insulator Composite Materials"

B. ONR Contract Number: N00014-85-K-0808

C. ONR Work Unit Number: 651-035

D. Principal Investigator: Dr. Robert P. Devaty
Graduate Students: Ralph E. Sherriff (Mellon Fellow)
Michael F. MacMillan

E. ONR Scientific Officer: Dr. Wallace A. Smith

F. Period Covered: 88JAN01-88DEC31

II. RESEARCH PERFORMED IN 1988

A. Infrared Properties of Thin Pt/Al_2O_3 Granular Metal-Insulator Composite Films

The infrared properties of thin Pt/Al_2O_3 granular metal-insulator composite films (cermets) were investigated using Fourier transform spectroscopy. The films were grown by dual electron beam evaporation onto polished single crystal sapphire substrates. They were barrowed from Dr. J.V. Mantese of General Motors Research Labs. The metallic volume fraction, which was controlled by the deposition conditions, ranged from 23% to 100% in the set of samples. The percolation threshold estimate from the temperature dependence of the dc resistance is greater than 50%, which implies that the Pt particles are highly correlated. The percolation threshold for a random metal-insulator mixture is less than 20%.

The transmission and relative reflection of the films were measured at room temperature using a Nicolet 740 Fourier transform infrared spectrometer (FTIR), which arrived at the beginning of the year. The mid and near infrared regions (400-15250 cm^{-1}) were covered using three combinations of sources, beamsplitters, and detectors. The reflection standard was a 100% Pt film from the sample set. The angle of incidence for the reflection measurements was 5^{o}.

The data were compared with three effective medium theories which describe distinct microstructural topologies: Maxwell-Garnett (dielectric-coated metal spheres), Bruggeman (metal and insulator treated on the same footing), and the Ping Sheng model (metal-coated dielectric and dielectric-coated metal spheres treated symmetrically). The Sheng model is in a sense a combination of the other two. It was developed specifically for application to cermet films. The underlying argument is based on a probabilistic growth mechanism for the films. The best available data on bulk optical properties were used to model the complex dielectric functions of the substrate and the film components.

The measured relative reflection for some of the samples is compared with the predictions of the three models in the accompanying preprint. Figures 1 and 2 show a comparison between the measured transmission and the predictions of the three models. Samples with greater than 50% Pt do not transmit well. Figure 3 shows the volume fraction dependence of the transmission at two selected frequencies. The Sheng model provides the best agreement with the data over the complete range of metallic composition, in agreement with the analysis of the relative reflection. Thus, the spectroscopic measurements suggest that the Pt particles in the films are correlated rather than randomly dispersed. No direct corroboration by a technique such as electron microscopy has been obtained.

The most striking disagreement between theory and experiment occurs near the dc percolation threshold, f_c. It is best observed in the reflection data. This result is not surprising as effective medium theories are known to fail near percolation. Details of cluster morphology not included in the effective medium treatments, such as nonspherical shape, are most important near f_c.

B. Far Infrared Properties of Small Bismuth Particles

Small bismuth particles were prepared by inert gas evaporation and dispersed in paraffin, which does not absorb strongly in the frequency range of interest. The far infrared absorption associated with the plasma sphere resonance in 1 μm diameter bismuth particles was measured, identified, and compared with a model we had developed earlier. The measured absorption coefficient, which peaks near 170 cm^{-1}, is enhanced by about a factor of five relative to the prediction.

The dependence of the plasma resonance absorption on particle size was studied. The resonance is not observed for samples with mean particle diameters less than .25 μm. Enhanced background absorption (i.e., weak frequency dependence) was observed for the smallest particles. Particle sizes were measured by transmission electron microscopy.

The far infrared transmission of a powder of 1 μm diameter free standing bismuth particles in a magnetic field was studied. A group of cyclotron-like resonances (resonance frequency approaches zero as the magnetic field is removed) was observed. The observed resonances confirmed earlier

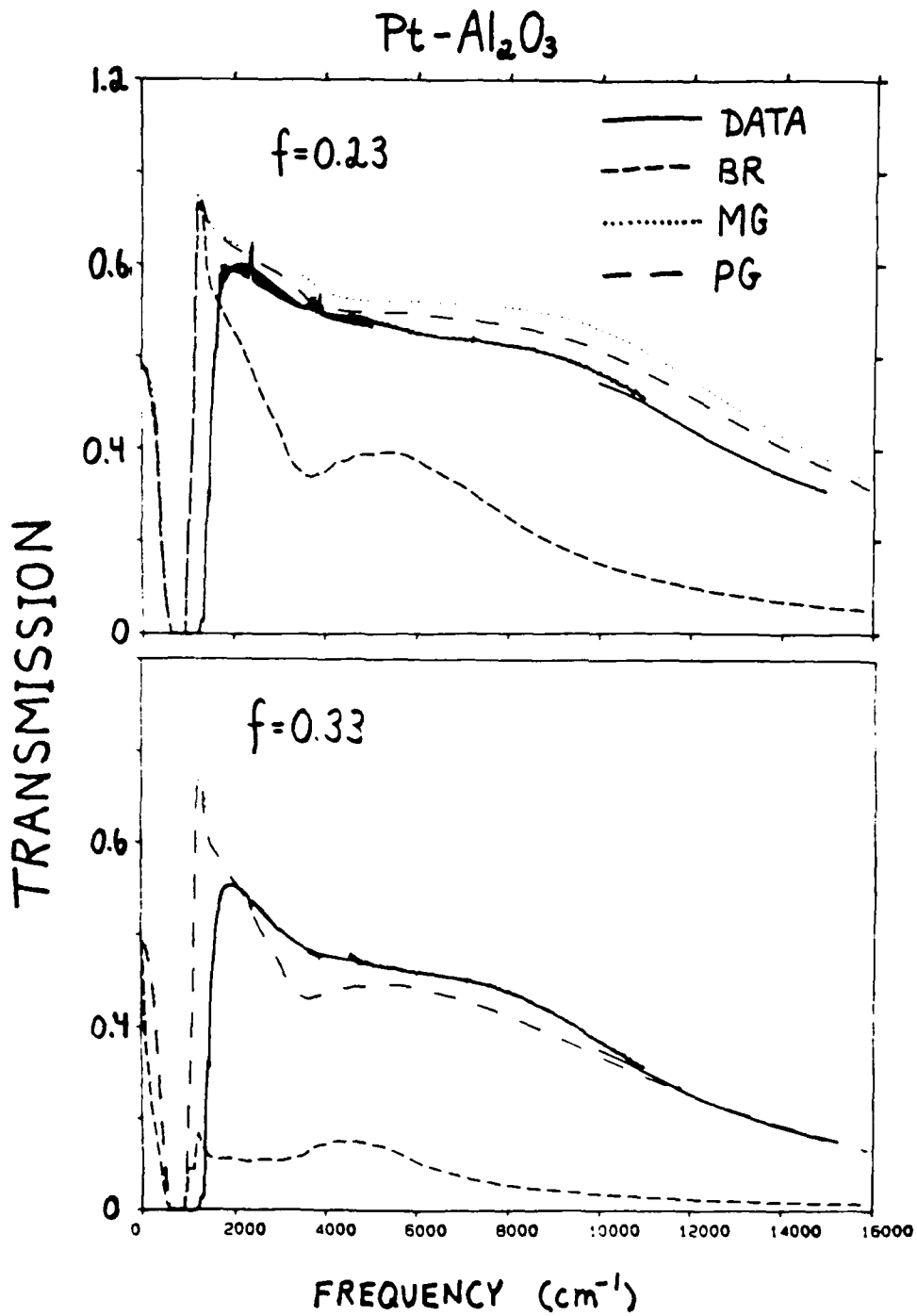

Figure 1. Transmission spectra of Pt-Al_2O_3 granular composite films. The predictions of the Maxwell-Garnett (MG), Bruggeman (BR) and Ping Sheng probabilistic growth (PG) models are also shown. The PG model describes the data best.

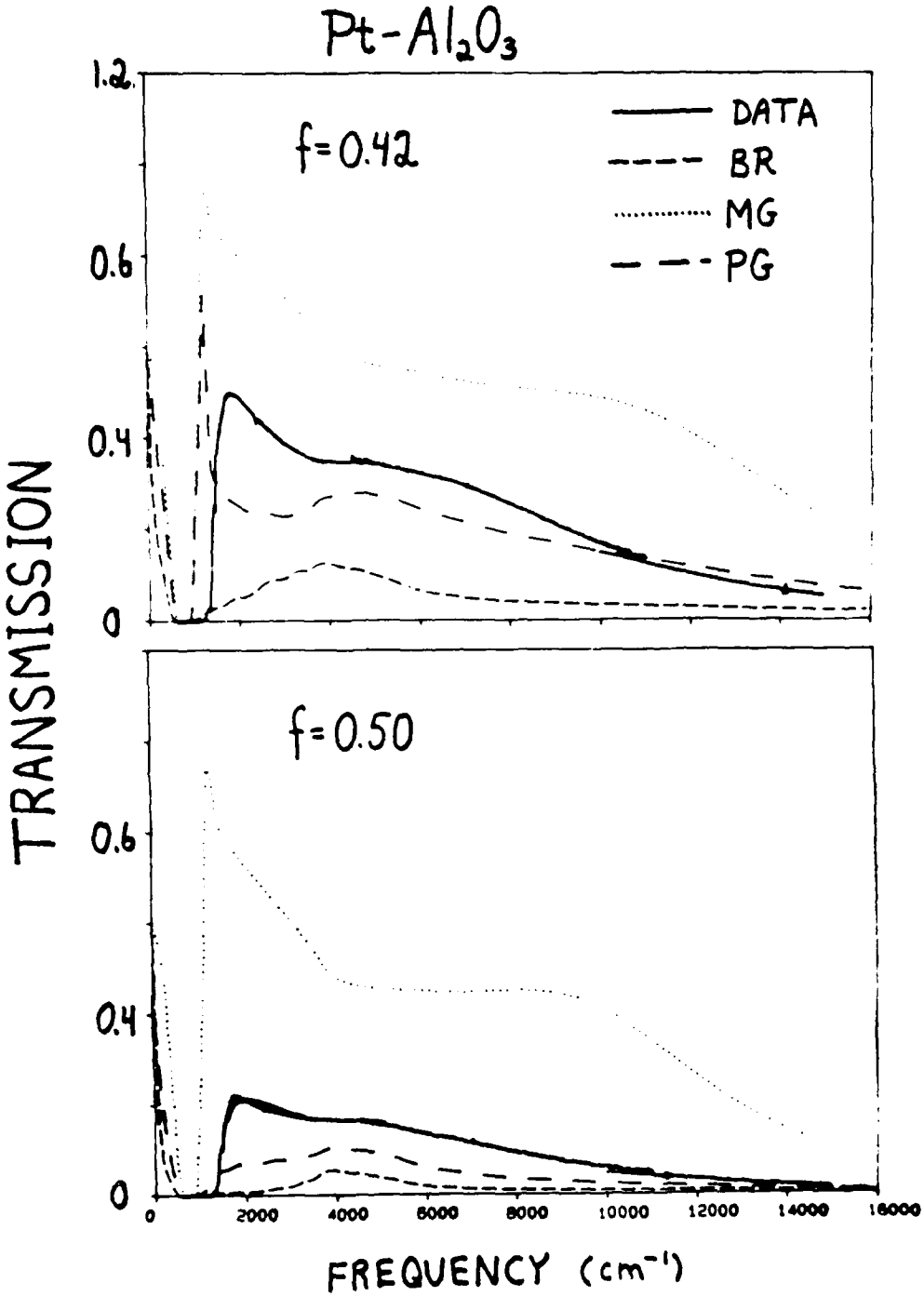

Figure 2. Transmission spectra of Pt-Al_2O_3 granular composite films. The predictions of the Maxwell-Garnett (MG), Bruggeman (BR) and Ping Sheng probabilistic growth (PG) models are also shown. The PG model describes the data best.

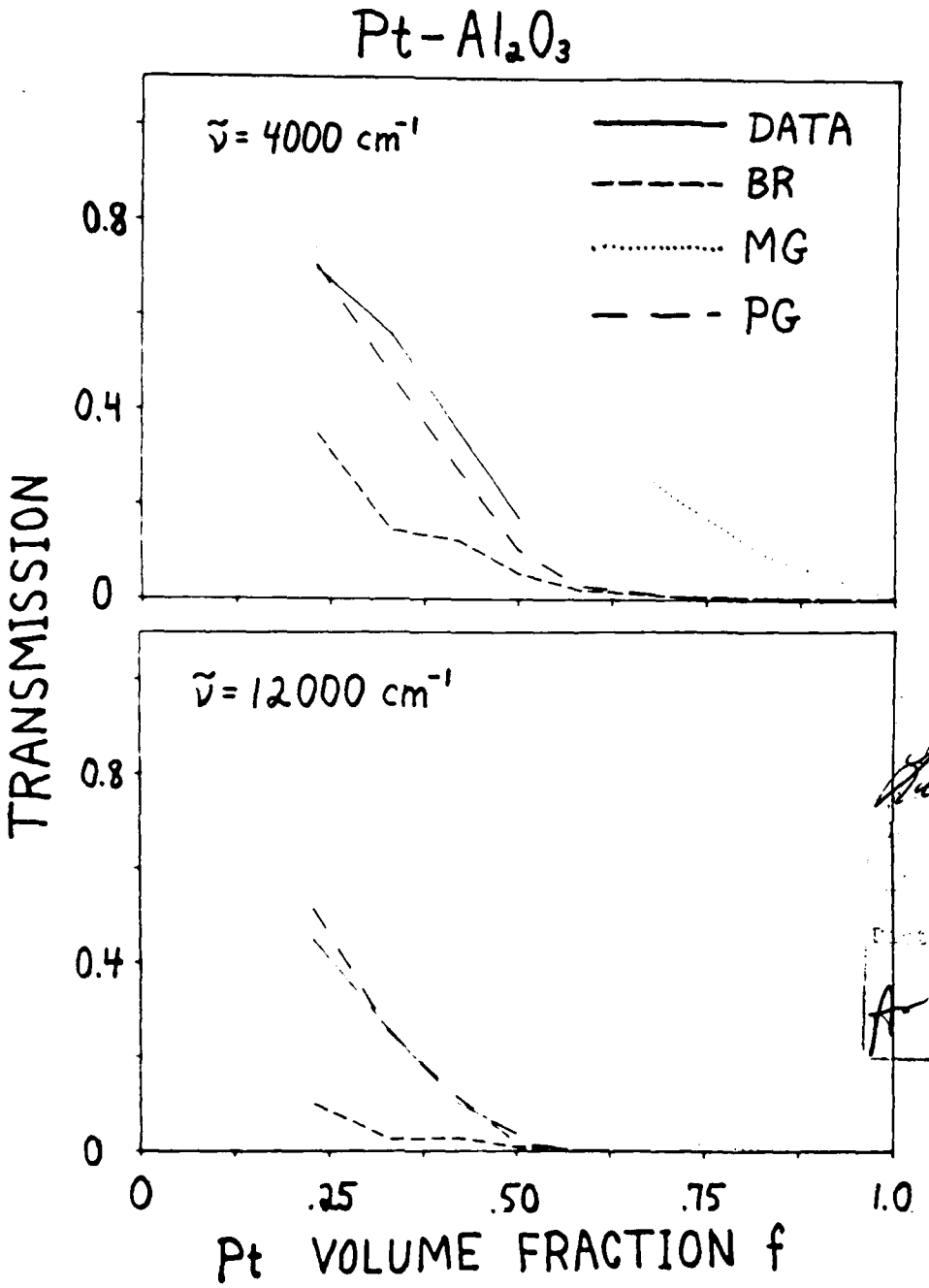

Figure 3. Volume fraction dependence of the infrared transmission of Pt-Al_2O_3 granular composite films at selected frequencies. Also shown are the predictions of the Maxwell-Garnett (MG), Bruggeman (BR) and Ping Sheng probabilistic growth (PG) models. The PG model best describes the data. The samples do not transmit above the percolation threshold, so the comparison shown here is only meaningful for relatively low metallic volume fractions.

unpublished experimental results of Chin and Sievers. In addition, we observed evidence for many more resonances in qualitative agreement with our model. Better data (higher resolution, improved sensitivity) are required to make the comparison quantitiative. We obtained evidence that the plasma sphere resonance is blue-shifted in a magnetic field, in agreement with theory. We performed the magnetooptical studies at Cornell University, where a cryostat with a superconducting solenoid is available.

Further details regarding the measurements on bismuth particles are given in the accompanying preprint. Many other details remain to be written up.

Our expressions for the extinction coefficient of a gyrotropic sphere in the long wavelength limit were applied to small bismuth particles in zero magnetic field. For the anisotropic dielectric tensor of bismuth, the expressions are not sufficiently general to treat the case of nonzero applied field. However, the average over particle orientations necessary to treat our samples is straightforward to perform.

Improvements in the far infrared system over the past year include the construction of an output coupler which uses mirrors to replace the TPX lens that came with the SPECAC interferometer. The intensity of modulated radiation emitted from the interferometer was increased, especially for frequencies greater than 200 cm^{-1}, a region of interest for bismuth. A new sample rotator insert, which permits multiple exchanges of samples with minimal accumulation of frozen air on the sapphire window which isolates the detector chamber from the rest of the cryostat, was constructed. A small dewar to house one of the composite silicon bolometers was purchased from Infrared Laboratories using startup money from the University. This dewar is convenient for diagnostics as well as room temperature transmission measurements. In addition, it is compatible with the Nicolet 740, for which it can be used to improve performance in the far infrared.

C. Theory

1. Magnetic Field-Induced Resonances in Small Spherical n-InSb Particles

As part of a continuing investigation of the interaction of electromagnetic waves with a small gyrotropic sphere, a simple model for magnetic field-induced resonances in an isotropic single-carrier polar semiconductor sphere was developed and applied to n-InSb. Free carriers were treated using the Drude model, which is characterized by the plasma frequency ω_p. The optic phonons were modeled by a Lorentz oscillator, for which the transverse and longitudinal frequencies are denoted ω_T and ω_L, respectively. Depending on the doping and temperature, one can have $\omega_p < \omega_T$, $\omega_T < \omega_p < \omega_L$, or $\omega_p > \omega_L$. Both electric dipole and magnetic dipole-electric quadrupole field dependent resonances are predicted in the long wavelength limit. To examine magnetic dipole-electric quadrupole resonances,

use is made of our recently derived general expressions for the gyrotropic sphere (See reprint). The behavior of the electric dipole resonances is similar to the well-known plasma shifted cyclotron resonances with additional coupling to the optic phonons (Figure 4).

2. The Effect of Clustering on the Far Infrared Absorption of Small Metal Particles: A Simple Model

Clustering of the particles plays an important role in the anomalous enhancement of the far infrared absorption coefficient of small metal particles, as was shown experimentally by several groups[1-3]. Curtin and Ashcroft[4] introduced a number of models which show how clusters of particles produce enhanced absorption. One of these, the cluster percolation model, applies to clusters of electrically isolated particles. The low conductivity of a cluster near the dc percolation threshold leads to the enhancement. The enhancement can be regarded as a resonance in the metallic volume fraction of the cluster, in analogy with the plasma sphere resonance in the frequency dependence of the optical properties an isolated small particle. Curtin and Ashcroft modeled their clusters using an approach based on the real space renormaliztion group. Here we examine a simpler model which produces a similar effect.

A cluster of particles is replaced by an homogeneous sphere made up of an effective medium. We choose to use the Bruggeman model for the effective dielectric function. This model has a percolation threshold, which is required to produce the enhancement. An actual sample will contain clusters with a range of metallic volume fractions, with perhaps only a small fraction near percolation. Like Curtin and Ashcroft, we assume that the details of the cluster distribution are unimportant and consider a distribution which is constant over a range of volume fractions that includes the percolation threshold. The volume fraction of metal in the sample is presumed to be much less than unity. We use the Maxwell-Garnett model in the dilute limit to obtain the effective dielectric function for the medium. In summary, effective medium theory has been applied twice: first to treat the clusters, then to treat the entire sample.

For dispersed particles the absorption coefficient is given by

$$\alpha(\tilde{\omega}) = 18\pi f \varepsilon_0^{1/2} \tilde{\omega} \frac{\varepsilon_2(\tilde{\omega})}{\left[\varepsilon_1(\tilde{\omega}) + 2\varepsilon_0\right]^2 + \varepsilon_2(\tilde{\omega})^2}.$$

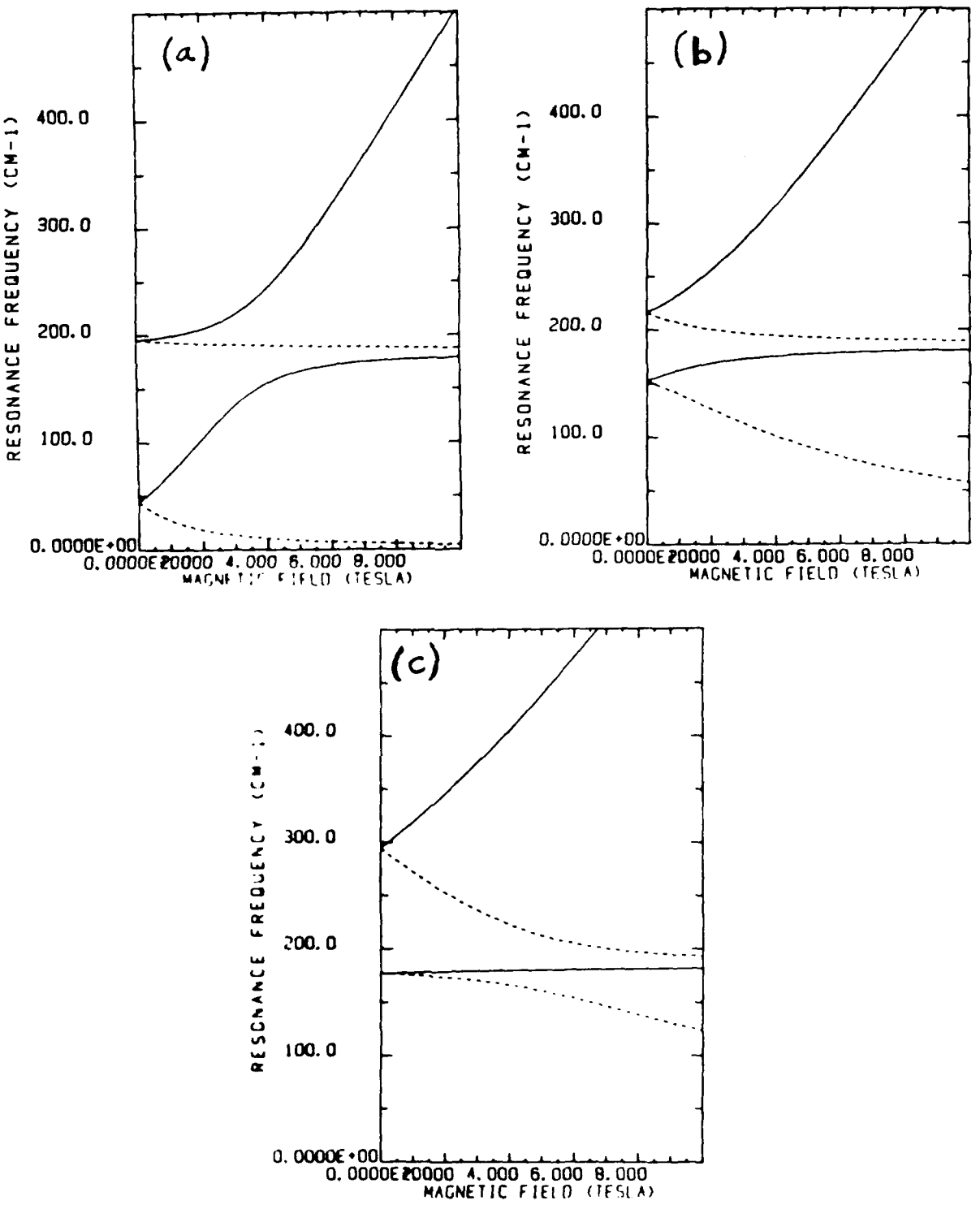

Figure 4. Magnetic field dependence of electric dipole resonances in small spherical n-InSb particles. The optic modes of InSb are included in the model. The solid lines indicate the "cyclotron resonance active" resonances, the dashed lines the "cyclotron inactive" resonances. The parameters used in the calculations were ω_L = 196 cm^{-1}, ω_T = 184 cm^{-1}, ε_L = 16, and m*/m = 0.019. The plasma frequency, which is determined by the carrier concentration is: a) ω_p = 50 cm^{-1}, b) ω_p = 190 cm^{-1}, and c) ω_p =300 cm^{-1}. The interaction between the plasma shifted cyclotron resonance and the optic phonons is significant near 200 cm^{-1}.

Here f is the volume fraction of metal, ε_1 and ε_2 are the real and imaginary parts of the complex dielectric function of the metal, ε_0 is the dielectric constant of the host, and $\tilde{\omega}$ is the frequency in wavenumbers. For clusters,

$$\alpha(\tilde{\omega}) = 18\pi f \varepsilon_0^{1/2} \tilde{\omega} \int \frac{dp\, P(p)\, \bar{\varepsilon}_2(\tilde{\omega};p)}{\left[\bar{\varepsilon}_1(\tilde{\omega};p) + 2\varepsilon_0\right]^2 + \bar{\varepsilon}_2(\tilde{\omega};p)^2}$$

where P(p) is the distribution of metallic volume fractions within the clusters and $\bar{\varepsilon}_1(\bar{\varepsilon}_2)$ is the real (imaginary) part of the complex effective dielectric function for a cluster.

The model is applied to 100 Å diameter silver particles in KCl. The parameters of the Drude model for silver are ω_p = 72,600 cm^{-1} (plasma frequency) and $1/\tau$ = 370 cm^{-1} (electron scattering rate due to the boundaries of the particles). The low frequency dielectric constant of KCl is ε_0 = 4.2. Figure 5 shows the predicted frequency dependence of the far infrared absorption coefficient for dispersed and clustered particles. In this case, clustering produces an enhancement of about a factor of ten.

III. RESEARCH PLANS FOR 1989

A. Infrared Properties of Pt/Al_2O_3 Cermet Films and Pt/KBr Pressed Pellets

We have started a study of the infrared reflection of pressed pellets of Pt particles (purchased Pt black) in KBr. A similar study[5] was performed on inert gas evaporated silver particles imbedded in KCl by a group at Ohio State several years ago. We choose to study Pt particles so that our results can be compared with our work on the Pt-Al_2O_3 cermet films. The two systems probably have very different microstructures. The particles in a cermet film are apparently correlated. In a pressed pellet, the particles should be randomly dispersed on some length scale. There may be clustering if repeated grinding and pressing does not produce an homogenous mixture. Cummings et al.[5] concluded that the Bruggeman model provides a good description of their data. It will be interesting to learn whether the percolation threshold of the pressed pellet system is below 20% metallic volume fraction, in agreement with theory for random mixtures and in contrast with the result for the cermet system.

In addition, there is a possibility of obtaining a new type of metal-insulator thin film composite system in the coming year through my collaboration with Dr. J.V. Mantese of General Motors Research Labs.

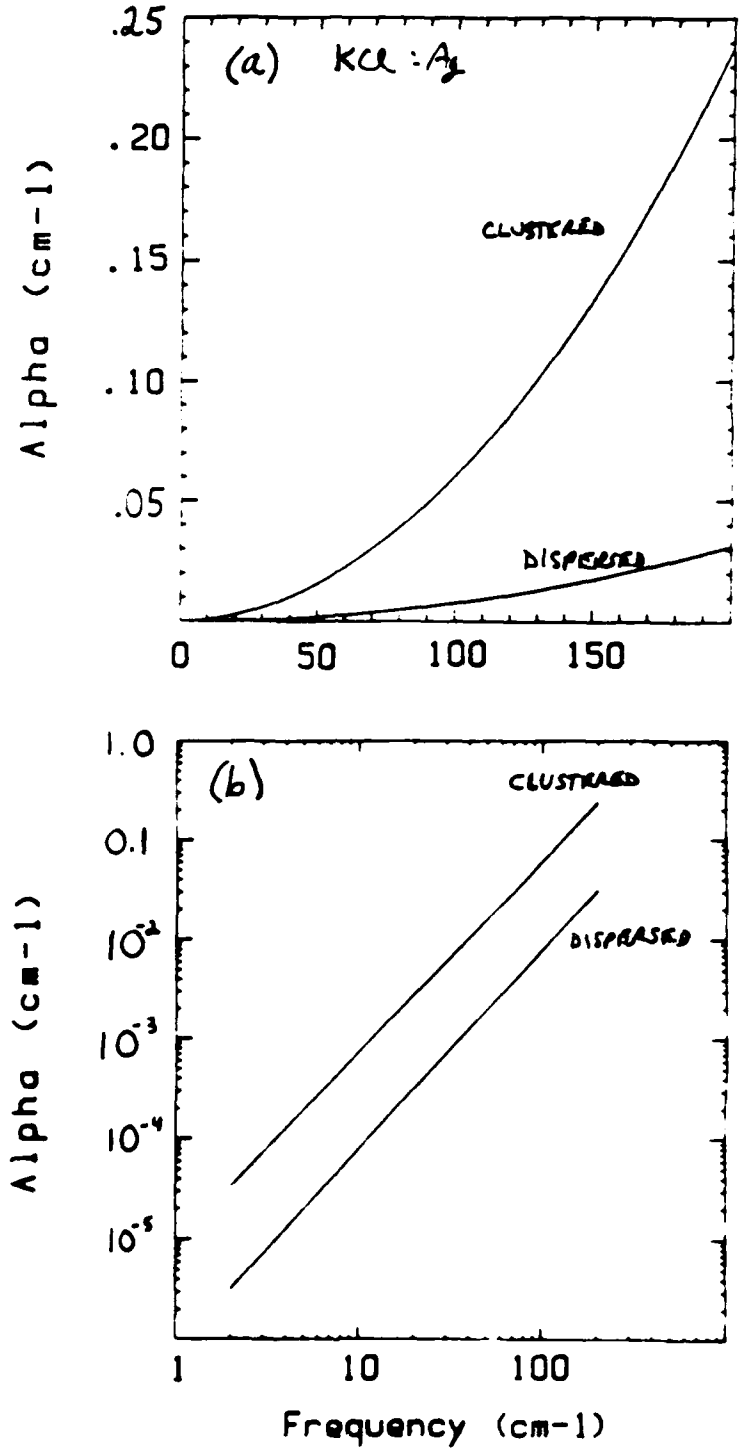

Figure 5. Effect of clustering on the far infrared absorption coefficient of 100 Å Ag particles embedded in KCl. The calculation is described in the text. For this simple model, an enhancement of about a factor of ten is predicted if the particles are clumped. a) linear plot b) log-log plot.

Theoretically, we have some interest in investigating the Sheng model. During a conversation at the Fall MRS Meeting, Ping Sheng pointed out that his model predicts an infrared plasma edge in the reflectivity of cermets that does not come out of the other oft-used effective medium theories. Will this effect be observable in composite systems based on Pt metal, which is non-Drude? For a Drude metal and a transparent host, the Sheng model predicts a great detail of structure in, e. g., the reflectivity that does not come out of the Maxwell-Garnett or Bruggeman models.

The possibility of applying new theoretical developments in the optical properties of metal-insulator composite materials, especially in the region near percolation, to the Pt-Al_2O_3 system will be investigated. Several interesing theoretical results based on scaling theories, the renormalization group, etc., were presented at the ETOPIM2 Conference in Paris last summer.

We plan to improve our measurements of the reflectivity of composite materials by measuring the absolute rather than relative reflectivity. We purchased a V-W reflectometer last year, but it has not been able to do the job thus far. We have continuing discussions on this device with Harrick Scientific Corp. and hope that the problems are resolved in the next few months. Once we can measure the absolute reflectivity, we plan to develop a computer program to convert transmission and reflection measurements on the thin cermet films to the optical constants n and k.

B. Far Infrared Properties of Small Bismuth Particles

Our proposal to the Defense-University Research Instrumentation Program (DURIP) has recently been selected for funding. A cyrostat with a superconducting magnet for far infrared magnetooptical studies and a far infrared laser will be purchased and installed this year. The magnetic field dependence of far infrared resonances in bismuth particles will be investigated and compared with the predictions of our model. An in-house facility for magnetooptics provides the opportunity for a thorough magnetooptical investigation of bismuth particles that was not possible when we were required to make short trips to Cornell.

Studies of the size dependence of the far infrared absorption in bismuth particles will continue. Besides the plasma sphere resonance, a new probe, an interband transition at higher frequencies, will become available if we are successful in developing a low temperature silicon window and if the bandwidth of the SPECAC interferometer is found to extend to sufficiently high frequencies. CsI will be examined as a potentially superior host material over paraffin at high frequencies. In coversations at the ETOPIM2 Conference in Paris, I learned that doping of bulk bismuth has been used to modify the concentration of carriers. If doped small particles of bismuth can be produced, the doping should strongly affect the far infrared resonances, both in a magnetic field and in zero field.

Improvements to the far infrared system will continue as the need arises.

References

1. R.P. Devaty and A.J. Sievers, Phys. Rev. Lett. 52, 1344 (1984).

2. W.A. Curtin, R.C. Spitzer, N.W. Ashcroft, and A. J. Sievers, Phys. Rev. Lett. 54, 1071 (1985).

3. S.-I. Lee, T.W. Noh, K. Cummings, and J.R. Gaines, Phys. Rev. Lett. 54, 1626 (1985).

4. W.A. Curtin and N.W. Ashcroft, Phys. Rev. B31, 3287 (1985).

5. K.D. Cummings, J.C. Garland, and D.B. Tanner, Phys. Rev. B30, 4170 (1984).

IV. INDEX OF TECHNICAL REPORTS

1. "Conference on the Electrical Transport and Optical Properties of Inhomogeneous Media" (ETOPIM2), to be published in European Scientific Notes.

V. INDEX OF PUBLICATIONS AND PRESENTATIONS

A. PUBLICATIONS (~~refereed~~) (INCLUDED)

1. "Extinction of electromagnetic waves by a small gyrotropic sphere, " R.P. Devaty, Phys. Rev. B38, 7972 (1988).
2. "Far infrared absorption by small bismuth particles," R.E. Sherriff and R.P. Devaty, accepted for publication by Physica A.
3. "Infrared absorption of inhomogeneous media with metallic inculsions," R.P. Devaty, accepted for publication by Physica A.
4. "Infrared properties of thin Pt/Al_2O_3 granular metal-insulator composite films," M.F. MacMillan, R.P. Devaty, and J.V. Mantese, accepted for publication by Materials Research Society Symposium Proceedings: Multicomponent Ultrafine Microstructures.

B. INVITED PRESENTATIONS

1. "Infrared absorption of inhomogeneous media with metallic inclusions," review presented at ETOPIM2 Conference (Electrical Transport and Optical Properties of Inhomogeneous Media), Paris, France, Aug. 29-Sept. 2, 1988.

C. CONTRIBUTED PRESENTATIONS

1. "Extinction cross section for a small gyrotropic sphere," R.P. Devaty, Bull. Am. Phys. Soc. 33, 282 (1988), American Physical Society Meeting, New Orleans, LA, March 21-25, 1988.
2. "Plasma resonance in small bismuth particles," R.E. Sherriff and R.P. Devaty, Bull. Am. Phys. Soc. 33, 282 (1988), American Physical Society Meeting, New Orleans, LA, March 21-25, 1988.
3. "Far-infrared absorption by small bismuth particles," R.E. Sherriff and R.P. Devaty, ETOPIM2 Conference, Paris, France, Aug. 29-Sept. 2, 1988.
4. "Infrared properties of thin Pt/Al_2O_3 granular metal-insulator composite films," M.F. MacMillan, R.P. Devaty, and J.V. Mantese, Fall Meeting of the Materials Research Society, Boston, MA, Nov. 28-Dec. 2, 1988.
5. "Magnetic field-induced resonances in small spherical n-InSb particles", to be presented at the APS March Meeting, St. Louis, MO, March 20-24, 1989.

Extinction of electromagnetic waves by a small gyrotropic sphere

R. P. Devaty
Department of Physics and Astronomy, University of Pittsburgh, Pittsburgh, Pennsylvania 15260
(Received 16 March 1988)

The general solution of Ford and Werner for the scattering and absorption of a plane electromagnetic wave by a gyrotropic sphere is analyzed in the long-wavelength limit. An expression is obtained for the extinction cross section which includes the electric dipole term as well as the magnetic dipole and electric quadrupole terms, which are coupled. The results agree with the Mie solution in the limit of vanishing gyrotropy. The expressions are applied to a lossless single-component plasma sphere. Agreement is obtained with recent work based on a quasistatic approximation.

I. INTRODUCTION

Recently Ford and Werner[1] presented a solution to the problem of the scattering and absorption of a plane electromagnetic wave by a gyrotropic sphere made up of material having a frequency-dependent complex dielectric tensor of the form

$$\vec{\epsilon}(\omega)=\begin{vmatrix} \epsilon_{xx} & \epsilon_{xy} & 0 \\ -\epsilon_{xy} & \epsilon_{xx} & 0 \\ 0 & 0 & \epsilon_{zz} \end{vmatrix} . \tag{1}$$

Gyrotropy is frequently introduced via a static uniform applied magnetic field **H**. Although not completely general, this tensor applies to microwave and far-infrared measurements on narrow-gap semiconductors[2-9] as well as electron-hole droplets in Ge (Refs. 10–23) for certain orientations of the crystal with respect to the applied magnetic field.

Approximate solutions which apply to particles that are much smaller than the wavelength of the electromagnetic radiation are important because they frequently apply to experiments and because the expressions obtained in this limit are relatively simple and accessible to physical interpretation. Consider the Mie-Debye problem[24,25] of scattering and absorption by an isolated homogeneous isotropic sphere ($\mathbf{H}=\mathbf{0}$) having radius a and complex dielectric function $\epsilon(\omega)$ embedded in a nonabsorbing host with dielectric constant ϵ_2. Define the dimensionless parameter

$$x \equiv ka = \epsilon_2^{1/2}\omega a/c \tag{2}$$

where ω is the frequency of the wave and k is the wave number. In the limit $x \ll 1$ the pair of infinite independent multipole series reduces to three terms, to order x^3. For example, the extinction cross section is[26,27]

$$\sigma_{\rm ext}=\sigma_1^{(e)}+\sigma_1^{(m)}+\sigma_2^{(e)} \tag{3}$$

where

$$\sigma_1^{(e)}=4\pi a^2 x\left\{\mathrm{Im}\left[\frac{\epsilon-\epsilon_2}{\epsilon+2\epsilon_2}\right]+\tfrac{3}{5}x^2\mathrm{Im}\left[\frac{(\epsilon-2\epsilon_2)(\epsilon-\epsilon_2)}{(\epsilon+2\epsilon_2)^2}\right]+\tfrac{2}{3}x^3\mathrm{Re}\left[\left[\frac{\epsilon-\epsilon_2}{\epsilon+2\epsilon_2}\right]^2\right]+O(x^4)\right\}, \tag{4a}$$

$$\sigma_1^{(m)}=\frac{2\pi}{15}a^2x^3\left[\mathrm{Im}\left[\frac{\epsilon}{\epsilon_2}-1\right]+O(x^2)\right], \tag{4b}$$

$$\sigma_2^{(e)}=\frac{2\pi}{3}a^2x^3\left[\mathrm{Im}\left[\frac{\epsilon-\epsilon_2}{2\epsilon+3\epsilon_2}\right]+O(x^2)\right] \tag{4c}$$

are the electric dipole, magnetic dipole, and electric quadrupole terms, respectively. For most situations the electric dipole term is the most important, and the magnetic dipole and electric quadrupole terms are the leading corrections.

In the long-wavelength limit, it is also possible to obtain expressions for the extinction coefficient and related quantities based on a quasistatic approximation. One can distinguish the condition $x \ll 1$, i.e., the wavelength of the incident wave in the host is much larger than the particle size, from the usually more restrictive condition that the wavelength inside the particle also be much greater than the size (the Rayleigh limit). The electromagnetic wave is approximated by uniform oscillating electric and magnetic fields. Retardation effects are ignored. The responses of the particle to the electric and magnetic fields are treated separately. The results agree with the electric and magnetic dipole terms of the Mie series to leading order in x. It is straightforward to generalize the quasistatic approximation for the electric dipole term to particles having ellipsoidal shape[28] and/or anisotropic dielectric tensor.[29] The quasistatic approximation also underlies the arguments leading to effective-medium theories[30,31] for composite materials.

Ford and Werner[1] obtained expressions for the electric and magnetic dipole moments for a gyrotropic sphere in the Rayleigh limit. Their expressions agree with results derived using a quasistatic approximation,[32-34] for which the electric and magnetic fields are assumed to decouple.

Furdyna *et al.*[35] and Goettig and Trzeciakowski[36] recently calculated the electromagnetic modes of oscillation

of a small, lossless, single-carrier, conducting sphere in a uniform static magnetic field. Their quasistatic approximation allowed for coupling of the electric and magnetic modes through displacements of the plasma with respect to the uniform compensating background. The modes possess nonvanishing surface and, in some cases, volume charge densities. The interaction of external electromagnetic radiation with these modes and the absorbed power were determined using a quantization scheme originally developed for the zero-field case.[37,38] The frequencies and power absorption for the electric dipole resonances are in agreement with earlier work,[32–34] but not for the magnetic dipole modes. The origin of the discrepancy is that the electric and magnetic fields do not decouple, contrary to the assumptions of the earlier work. In the long-wavelength limit, the magnetic dipole and electric quadrupole terms, which are of the same order in x, mix. This mixing was also recognized in some of the earlier work.[1,7]

The question remains as to why the long-wavelength limit of the Ford-Werner (FW) solution agrees with the older incorrect quasistatic approximation rather than the recent results of Furdyna *et al.*[35] and Goettig and Trzeciakowski.[36] In this paper, we obtain the correct expressions from the FW theory for the magnetic dipole-electric quadrupole extinction cross sections in the long-wavelength limit. In effect we are generalizing Eqs. (4b) and (4c) to the gyrotropic case. We do not treat corrections to the electric dipole absorption that are of the same order as the magnetic-dipole–electric-quadrupole terms. In addition to resolving the discrepancy, this work generalizes the results of Furdyna *et al.*[35] and Goettig and Trzeciakowski[36] to any dielectric tensor given by Eq. (1). Multicomponent plasmas, phenomenological damping, interband absorption, etc. may be included in the treatment. The restrictions are those of the long-wavelength limit. In cases of doubt one should make use of the full FW theory.

The paper is organized as follows. Section II presents the derivation of the extinction coefficient from the FW theory in the long-wavelength limit. Although it is well understood, the electric dipole term is included for completeness. Section III discusses the results in the context of previous work on the single-component Drude plasma. Section IV summarizes the conclusions.

II. EXTINCTION COEFFICIENT IN THE LONG-WAVELENGTH LIMIT

Ford and Werner[1] write the extinction cross section as [Eq. (2.59) in their paper]

$$\sigma_{\text{ext}}=\frac{4\pi}{k}\text{Im}[\mathbf{F}(\hat{\mathbf{k}},\hat{\mathbf{k}})\cdot\mathbf{E}_1^*/|\mathbf{E}_1|^2] \tag{5}$$

where $\mathbf{F}(\hat{\mathbf{k}}_1,\hat{\mathbf{k}}_2)$ is the vector scattering amplitude [Eq. (FW3.49)], $\hat{\mathbf{k}}$ is a unit vector pointing in the direction of propagation of the electromagnetic wave, and $\mathbf{E}_1$ is the electric field vector of the incident wave. The asterisk denotes complex conjugation. Equations from the paper by Ford and Werner[1] are indicated by the prefix FW. The quantity of greatest interest here is $Z_{ll'}^{m\sigma}$, the ratio of $N\times N$ determinants that appears in $\mathbf{F}(\hat{\mathbf{k}},\hat{\mathbf{k}})$. For example [from Eq. (FW3.47)],

$$Z_{l1}=\begin{vmatrix} Y_{l1} & Y_{l2} & Y_{l3} & \cdots \\ X_{21} & X_{22} & X_{23} & \cdots \\ X_{31} & X_{32} & X_{33} & \cdots \\ \vdots & \vdots & \vdots & \end{vmatrix} \Big/ \begin{vmatrix} X_{11} & X_{12} & X_{13} & \cdots \\ X_{21} & X_{22} & X_{23} & \cdots \\ X_{31} & X_{32} & X_{33} & \cdots \\ \vdots & \vdots & \vdots & \end{vmatrix} \tag{6}$$

where the expressions for $X_{lk}^{m\sigma}$ and $Y_{lk}^{m\sigma}$ are given by Eqs. (FW3.35) and (FW3.39). The indices m and σ are suppressed in Eq. (6). For details on the FW theory, definitions, and notation the reader is referred to the original paper.[1]

Ford and Werner[1] calculated the electric and magnetic dipole moments of the gyrotropic sphere in the long-wavelength limit. Their results can be used to compute the extinction cross section and related quantities. Their expression for the electric dipole term is correct, but further examination of the magnetic dipole term is required. (1) Due to mixing with the electric quadrupole term, additional terms of the same order must be considered. (2) The assumption $x \ll y$, where $y \equiv qa$ with q a parameter analogous to the wave vector inside the sphere [Eq. (FW3.12)], is not required and in fact is the source of the disagreement of computed resonance frequencies with Furdyna *et al.*[35] and Goettig and Trzeciakowski.[36] We obtain the extinction cross section from Eq. (FW3.49).

Consider the eight terms in Eq. (FW3.49) with $l,l' \le 2$. Represent the indices l, l', m, and σ by (l,l',m,σ). Then $(1,1,m,+)$ denotes the electric dipole term. It is the lowest-order term in x and thus is expected to produce the largest extinction. The next term, $(1,1,m,-)$, is the magnetic dipole term. Although at first glance it appears to be of the same order as the electric dipole term, it is in fact of order x^3 because Z_{11}^{m-} is of order x^2. The term $(2,2,m,-)$, the electric quadrupole term, is also of order x^3. The terms $(1,2,m,-)$ and $(2,1,m,-)$ are of order x^3 and represent the interaction between the electric quadrupole and magnetic dipole terms. Therefore, all four terms should be considered together. In the limit of vanishing gyrotropy (e.g., isotropic material with no dc applied magnetic field), the cross terms vanish. The terms $(1,2,m,+)$, $(2,1,m,+)$, and $(2,2,m,+)$ are of higher order in x and will be neglected. They represent the magnetic quadrupole term and its coupling to the higher-order corrections to the electric dipole term in the long-wavelength limit.

A. Electric dipole term

The extinction cross section for the electric dipole term, or equivalent expressions such as the electric dipole moment, power absorption, and absorption coefficient, have been given correctly to lowest order by a number of authors.[1,32–34,39,40] We give the expressions here for completeness, but do not present the derivation, which is similar to that presented below for the magnetic-dipole–electric-quadrupole terms. The approach followed by FW is also correct.

We find that

$$Z_{11}^{m+}=\begin{cases}-2\dfrac{\epsilon_{zz}-\epsilon_2}{\epsilon_{zz}+2\epsilon_2}, & m=0\\ -2\dfrac{\epsilon_{\pm}-\epsilon_2}{\epsilon_{\pm}+2\epsilon_2}, & m=\pm1\end{cases} \tag{7}$$

where $\epsilon_{\pm}\equiv\epsilon_{xx}\pm i\epsilon_{xy}$. Since

$$[\mathbf{Y}_{11}^{m}(\hat{\mathbf{k}})^{*}\times\hat{\mathbf{k}}\cdot\mathbf{E}_1][\mathbf{Y}_{11}^{m}(\hat{\mathbf{k}})\times\hat{\mathbf{k}}\cdot\mathbf{E}_1^{*}/|\mathbf{E}_1|^2]=\frac{3}{8\pi}|\hat{\mathbf{e}}_m^{*}\cdot\hat{\mathbf{E}}_1|^2 \tag{8}$$

where $\hat{\mathbf{E}}_1\equiv\mathbf{E}_1/|\mathbf{E}_1|$,

$$\sigma_1^{(e)}=4\pi a^2 x\ \mathrm{Im}\begin{cases}\dfrac{\epsilon_{zz}-\epsilon_2}{\epsilon_{zz}+2\epsilon_2}, & m=0\\ \dfrac{\epsilon_{\pm}-\epsilon_2}{\epsilon_{\pm}+2\epsilon_2}, & m=\pm1\ .\end{cases} \tag{9}$$

B. Magnetic-dipole–electric-quadrupole terms

We present a detailed derivation for the long-wavelength limit of the magnetic dipole term. The derivations for the other terms of the same order are similar. The results are summarized in Table I.

From Eqs. (5) and (FW3.49) the contribution to the extinction cross section due to the magnetic dipole term $(1,1,m,-)$ is

$$\sigma_1^{(m)}=\frac{16\pi^2}{3}a^2x\ \mathrm{Im}\left\{\sum_{m=-1}^{1}Z_{11}^{m-}[\mathbf{Y}_{11}^{m}(\hat{\mathbf{k}})^{*}\times\hat{\mathbf{k}}\cdot\mathbf{B}_1]\times[\mathbf{Y}_{11}^{m}(\hat{\mathbf{k}})\times\hat{\mathbf{k}}\cdot\mathbf{B}_1^{*}/|\mathbf{B}_1|^2]\right\}, \tag{10}$$

where the $\mathbf{Y}_{11}^{m}(\hat{\mathbf{k}})$ are vector spherical harmonics.[34,41–43] Since

$$\mathbf{Y}_{11}^{m}(\hat{\mathbf{k}})=-i\left(\frac{3}{8\pi}\right)^{1/2}\hat{\mathbf{k}}\times\hat{\mathbf{e}}_m \tag{11}$$

and $\hat{\mathbf{k}}\cdot\mathbf{B}_1=0$,

$$[\mathbf{Y}_{11}^{m}(\hat{\mathbf{k}})^{*}\times\hat{\mathbf{k}}\cdot\mathbf{B}_1][\mathbf{Y}_{11}^{m}(\hat{\mathbf{k}})\times\hat{\mathbf{k}}\cdot\mathbf{B}_1^{*}/|\mathbf{B}_1|^2]=\frac{3}{8\pi}|\hat{\mathbf{e}}_m^{*}\cdot\hat{\mathbf{B}}_1|^2\ . \tag{12}$$

Now consider Z_{11}^{m-}, which is defined by Eq. (6). Since both $x\ll1$ and $y\ll1$, we shall expand in these two small parameters. Unlike FW we shall not impose $x\ll y$. We require the expansions of the spherical functions:[44]

$$j_1(x)\simeq\frac{x}{3}\left[1-\frac{x^2}{10}+\cdots\right], \tag{13a}$$

$$j_2(x)\simeq\frac{x^2}{15}\left[1-\frac{x^2}{14}+\cdots\right], \tag{13b}$$

TABLE I. $Z_{ll'}^{m\sigma}$, long-wavelength limit.

(l,l',σ)	$m=0$	$m=\pm1$	$m=\pm2$
$(1,1,+)$	$-2\dfrac{\epsilon_{zz}-\epsilon_2}{\epsilon_{zz}+2\epsilon_2}$	$-2\dfrac{\epsilon_{\pm}-\epsilon_2}{\epsilon_{\pm}+2\epsilon_2}$	
$(1,1,-)$	$\dfrac{1}{15}\left(\dfrac{\omega a}{c}\right)^2\dfrac{\epsilon_2[2\epsilon_+\epsilon_-+\epsilon_{xx}\epsilon_{zz}-\epsilon_2(2\epsilon_{xx}+\epsilon_{zz})]+2\epsilon_+\epsilon_-\epsilon_{zz}}{\epsilon_2(2\epsilon_{xx}+\epsilon_{zz})+2\epsilon_{xx}\epsilon_{zz}}$	$\dfrac{1}{30}\left(\dfrac{\omega a}{c}\right)^2\dfrac{\epsilon_2(\epsilon_{\pm}+\epsilon_{zz}-6\epsilon_2)+4\epsilon_{\pm}\epsilon_{zz}}{3\epsilon_2+\epsilon_{\pm}+\epsilon_{zz}}$	
$(1,2,-)$	$\dfrac{1}{2\sqrt{5}}\left(\dfrac{\omega a}{c}\right)\dfrac{\epsilon_2(\epsilon_+-\epsilon_-)\epsilon_{zz}}{\epsilon_2(2\epsilon_{xx}+\epsilon_{zz})+2\epsilon_{xx}\epsilon_{zz}}$	$\pm\left(\dfrac{3}{20}\right)^{1/2}\left(\dfrac{\omega a}{c}\right)\dfrac{\epsilon_2(\epsilon_{\pm}-\epsilon_{zz})}{3\epsilon_2+\epsilon_{\pm}+\epsilon_{zz}}$	
$(2,1,-)$	$-\dfrac{\sqrt{5}}{6}\left(\dfrac{\omega a}{c}\right)\dfrac{(\epsilon_+-\epsilon_-)\epsilon_{zz}}{\epsilon_2(2\epsilon_{xx}+\epsilon_{zz})+2\epsilon_{xx}\epsilon_{zz}}$	$\mp\left(\dfrac{5}{12}\right)^{1/2}\left(\dfrac{\omega a}{c}\right)\dfrac{\epsilon_{\pm}-\epsilon_{zz}}{3\epsilon_2+\epsilon_{\pm}+\epsilon_{zz}}$	
$(2,2,-)$	$\dfrac{\epsilon_2(2\epsilon_{xx}+\epsilon_{zz})-3\epsilon_{xx}\epsilon_{zz}}{\epsilon_2(2\epsilon_{xx}+\epsilon_{zz})+2\epsilon_{xx}\epsilon_{zz}}$	$\dfrac{3}{2}\dfrac{2\epsilon_2-\epsilon_{\pm}-\epsilon_{zz}}{3\epsilon_2+\epsilon_{\pm}+\epsilon_{zz}}$	$3\dfrac{\epsilon_2-\epsilon_{\pm}}{3\epsilon_2+2\epsilon_{\pm}}$

$$h_1^{(1)}(x)\simeq -\frac{i}{x^2}\left[1+\frac{x^2}{2}+\cdots\right], \tag{13c}$$

$$h_2^{(1)}(x)\simeq -\frac{3i}{x^3}\left[1+\frac{x^2}{6}+\cdots\right], \tag{13d}$$

as well as the expansions for $\alpha_1(x)$, $\alpha_2(x)$, $\alpha_1^{(1)}(x)$, and $\alpha_2^{(1)}(x)$, which are defined by Eq. (FW2.38). The procedure is to expand the matrices for Z_{11}^{m-} in x and y and manipulate the first and second rows of both the numerator and denominator matrices. The two matrices can be made identical to within factors of λ_k (i.e., y) and thus cancel, leaving a relatively simple result. The expansions of the row elements are

$$X_1^{m-}(\lambda)\simeq\left[1-\frac{x^2}{3}-\frac{y^2}{6}\right]d_{1m}^{-}(\lambda), \tag{14a}$$

$$Y_1^{m-}(\lambda)\simeq -\tfrac{1}{15}(x^2-y^2)d_{1m}^{-}(\lambda), \tag{14b}$$

$$X_2^{m-}(\lambda)\simeq\left[\frac{\omega a}{c}\right]\left[\frac{y^2}{15x^2}\left[1-\frac{y^2}{14}\right]\times\left[2d_{2m}^{-}(\lambda)-\frac{\epsilon_2}{\tilde{\epsilon}}\Delta_{2m}^{-}(\lambda)\right]+\frac{1}{5}\left[1-\frac{29y^2}{126}\right]d_{2m}^{-}(\lambda)\right]. \tag{14c}$$

Further manipulation is required for Eq. (14c). From the eigenvalue equation (FW3.15) we obtain

$$d_{2m}^{-}(\lambda)=-\left[\frac{5}{4-m^2}\right]^{1/2}\times\left[\frac{-m^2\bar{\gamma}+im\tilde{W}-2i\lambda\tilde{W}}{m\bar{\gamma}+i\tilde{W}}\right]d_{1m}^{-}(\lambda). \tag{15}$$

From the definition of $\Delta_{lm}^{\sigma}(\lambda)$ [Eq. (FW3.21)],

$$\Delta_{2m}^{-}(\lambda)=\tfrac{1}{2}[5(4-m^2)]^{1/2}(\bar{\gamma}m+i\tilde{W})d_{1m}^{-}(\lambda)+3\left[\bar{\gamma}\left[\frac{m^2-4}{6}\right]+\tfrac{1}{2}im\tilde{W}-i\lambda\tilde{W}\right]d_{2m}^{-}(\lambda). \tag{16}$$

From the definition of λ [Eq. (FW3.12)],

$$(1-i\lambda\tilde{W})=\frac{\tilde{\epsilon}}{y^2}\left[\frac{\omega a}{c}\right]^2. \tag{17}$$

$\tilde{W}$, $\bar{\gamma}$, and $\tilde{\epsilon}$ are defined by Eq. (FW3.2). After substitution and algebraic manipulation,

$$X_2^{m-}(\lambda)\simeq -\frac{2}{15}\frac{c}{\epsilon_2\omega a}\left[\frac{5}{4-m^2}\right]^{1/2}\times\frac{1}{m\bar{\gamma}+i\tilde{W}}(C_m x^2-A_m y^2)d_{1m}^{-}(\lambda) \tag{18}$$

where

$$C_m\equiv 2\frac{\tilde{\epsilon}}{\epsilon_2}-\left[\frac{m^2-4}{2}\right]\bar{\gamma}-\tfrac{1}{2}im\tilde{W}+3 \tag{19}$$

and

$$A_m\equiv(2+m^2\bar{\gamma}-im\tilde{W})+\frac{3}{4}\frac{\epsilon_2}{\tilde{\epsilon}}\left\{\left[2+\left[\frac{4-m^2}{3}\right]\bar{\gamma}-im\tilde{W}\right]\times(2+m^2\bar{\gamma}-im\tilde{W})-\tfrac{1}{3}(4-m^2)(m\bar{\gamma}+i\tilde{W})^2\right\}. \tag{20}$$

Next, we rearrange the numerator determinant by modifying the first row according to

$$Y_1^{m-}\rightarrow Y_1^{m-}-\frac{\epsilon_2\omega a}{2c}\left[\frac{4-m^2}{5}\right]^{1/2}(m\bar{\gamma}+i\tilde{W})C_m^{-1}X_2^{m-} \tag{21}$$

to obtain

$$Y_1^{m-}\simeq\frac{y^2}{15}(1-A_m/C_m)d_{1m}^{-}. \tag{22}$$

Similarly, modify the first row of the denominator determinant according to

$$X_1^{m-}\rightarrow X_1^{m-}+\frac{15}{2}\left[\frac{c}{\omega a}\right]\left[\frac{4-m^2}{5}\right]^{1/2}(m\bar{\gamma}+i\tilde{W})\times C_m^{-1}\left[1-\frac{x^2}{3}\right]X_2^{m-} \tag{23}$$

to obtain

$$X_1^{m-}\simeq\frac{A_m}{C_m}\frac{y^2}{x^2}d_{1m}^{-}(\lambda) \tag{24}$$

to lowest order.

Factors independent of λ can be factored from the first row of each determinant, leaving the numerator and denominator determinants equal, so that they cancel. Thus, in the long-wavelength limit,

$$Z_{11}^{m-}=\frac{\epsilon_2}{15}\left[\frac{\omega a}{c}\right]^2\left[\frac{C_m}{A_m}-1\right]. \tag{25}$$

Substitution for A_m and C_m leads to the result

$$Z_{11}^{m-}=\begin{cases}\dfrac{1}{15}\left[\dfrac{\omega a}{c}\right]^2\dfrac{\epsilon_2[2\epsilon_+\epsilon_--\epsilon_{xx}\epsilon_{zz}-\epsilon_2(2\epsilon_{xx}+\epsilon_{zz})]+2\epsilon_+\epsilon_-\epsilon_{zz}}{\epsilon_2(2\epsilon_{xx}+\epsilon_{zz})+2\epsilon_{xx}\epsilon_{zz}}, & m=0\\ \dfrac{1}{30}\left[\dfrac{\omega a}{c}\right]^2\dfrac{\epsilon_2(\epsilon_\pm+\epsilon_{zz}-6\epsilon_2)+4\epsilon_\pm\epsilon_{zz}}{3\epsilon_2+\epsilon_\pm+\epsilon_{zz}}, & m=\pm1\ .\end{cases}\tag{26}$$

We now summarize the results. The extinction cross section which we have calculated in the long-wavelength limit is

$$\sigma_{\rm ext}=\frac{(4\pi a)^2}{x}\,{\rm Im}\left[\sum_{l,l'}\sum_{m,\sigma}\frac{(-ix)^l}{(2l+1)!!}\frac{(ix)^{l'}}{(2l'-1)!!}Z_{ll'}^{m\sigma}\Phi_{ll'}^{m\sigma}(\hat{\mathbf{k}})\right]\tag{27}$$

where the summations are over the values of l, l', m, and σ discussed previously, and

$$\Phi_{ll'}^{m\sigma}(\hat{\mathbf{k}})\equiv\begin{Bmatrix}\mathbf{Y}_{l'l'}^{m}(\hat{\mathbf{k}})^*\times\hat{\mathbf{k}}\cdot\mathbf{B}_1, & \sigma=(-1)^{l'}\\ -\mathbf{Y}_{l'l'}^{m}(\hat{\mathbf{k}})^*\times\hat{\mathbf{k}}\cdot\mathbf{E}_1, & \sigma=(-1)^{l'+1}\end{Bmatrix}\times\begin{Bmatrix}\mathbf{Y}_{ll}^{m}(\hat{\mathbf{k}})\times\hat{\mathbf{k}}\cdot\mathbf{E}_1^*/|\mathbf{E}_1|^2, & \sigma=(-1)^{l+1}\\ \mathbf{Y}_{ll}^{m}(\hat{\mathbf{k}})\times\hat{\mathbf{k}}\cdot\mathbf{B}_1^*/|\mathbf{B}_1|^2, & \sigma=(-1)^{l}\end{Bmatrix}.\tag{28}$$

Also, $l!!\equiv1(1-2)(1-4)\cdots$.

Table I lists the expressions for $Z_{ll'}^{m\sigma}$. The $\Phi_{ll'}^{m\sigma}(\hat{\mathbf{k}})$ can be evaluated using

$$\mathbf{Y}_{11}^{m*}(\hat{\mathbf{k}})\times\hat{\mathbf{k}}\cdot\mathbf{E}_1=i\left[\frac{3}{8\pi}\right]^{1/2}(\hat{\mathbf{e}}_m^*\cdot\mathbf{E}_1)\ ,\tag{29a}$$

$$\mathbf{Y}_{22}^{m*}(\hat{\mathbf{k}})\times\mathbf{k}\cdot\mathbf{E}_1=\begin{cases}i\left[\dfrac{15}{8\pi}\right]^{1/2}k_0E_0, & m=0\\ i\left[\dfrac{5}{8\pi}\right]^{1/2}(k_\pm E_0+k_0E_\pm), & m=\pm1\\ i\left[\dfrac{5}{4\pi}\right]^{1/2}k_\pm E_\pm, & m=\pm2\end{cases}\tag{29b}$$

where

$$k_\pm\equiv\mp2^{-1/2}(k_x\mp ik_y)\ ,\qquad k_0\equiv k_z\ .\tag{30}$$

III. DISCUSSION

The expressions which we have derived correctly reduce to known results under the appropriate conditions. The extinction cross section reduces to the prediction of Mie theory [Eqs. (3) and (4)] when the source of gyrotropy is removed and the complex dielectric function of the sphere is assumed isotropic. In particular, we set $\epsilon_{xx}=\epsilon_{zz}\equiv\epsilon$, $\epsilon_{xy}=0$. The cross terms $(1,2,m,-)$ and $(2,1,m,-)$ vanish.

The frequencies of resonances induced by gyrotropy are obtained from the zeroes of the real parts of the denominators of the expressions in Table I. For a given value of m, the denominators for the magnetic dipole, electric quadrupole, and cross terms are the same. Therefore, only one of these terms need be considered for the evaluation of the resonance frequencies, but all are required to determine the strength of the resonances.

To proceed further it is convenient to specify a model for the complex dielectric function of the sphere. The simplest model consistent with Eq. (1) is a single-component Drude plasma in a uniform static applied magnetic field $\mathbf{H}=H\hat{\mathbf{z}}$. The diagonalized dielectric tensor is given by

$$\epsilon_\pm(\omega)=\epsilon_1\left[1-\frac{\omega_p^2}{\omega(\bar{\omega}\pm\omega_c)}\right],\tag{31a}$$

$$\epsilon_{zz}(\omega)=\epsilon_1\left[1-\frac{\omega_p^2}{\omega\bar{\omega}}\right]\tag{31b}$$

where

$$\omega_p\equiv\left[\frac{4\pi ne^2}{\epsilon_1 m^*}\right]^{1/2}\tag{32}$$

is the plasma frequency, n is the carrier density, e is the charge, m^* is the effective mass, and ϵ_1 the dielectric constant due to core polarizability. Also, $\omega_c\equiv eH/(m^*c)$ is the cyclotron frequency and $\bar{\omega}\equiv\omega+i/\tau$ where τ is the electronic scattering time. For a lossless Drude plasma, $\tau\to\infty$ and $\bar{\omega}\to\omega$. This case was studied by Furdyna *et al.*[35] and Goettig and Trzeciakowski.[36]

The electric dipole resonances are given by

$${\rm Re}[\epsilon_{zz}(\omega)+2\epsilon_2]=0\tag{33}$$

for $m=0$, which leads to

$$\omega_{101}=\omega_p\left[\frac{\epsilon_1}{2\epsilon_2+\epsilon_1}\right]^{1/2}\equiv\omega_1\tag{34}$$

for the resonance frequency. This frequency, which is independent of the applied magnetic field, is the resonance frequency for electric dipole plasma motion in zero field. The resonances are labeled according to the notation of Furdyna *et al.*[35] A resonance is labeled $\omega_{lm\tau}$, where $\tau=1$ if the frequency tends to ω_l, the lth zero-field mode of oscillation, in the low-field limit and $\tau=2$ if the frequency tends to zero. For $m=\pm1$, we set

$${\rm Re}[\epsilon_\pm(\omega)+2\epsilon_2]=0\tag{35}$$

to obtain

$$\omega_{1,\pm 1,1}=\mp\frac{\omega_c}{2}+\left[\left[\frac{\omega_c}{2}\right]^2+\omega_1^2\right]^{1/2} . \quad (36)$$

This result is the well-known plasma-shifted cyclotron resonance,[32,40,45,46] which describes the interaction between the cyclotron resonance and plasmon modes.

The magnetic-dipole–electric-quadrupole terms are considered together. For $m=0$, resonances are located from

$$\mathrm{Re}[\epsilon_2(2\epsilon_{xx}+\epsilon_{zz})+2\epsilon_{xx}\epsilon_{zz}]=0 . \quad (37)$$

The resonance frequencies are the two real positive solutions of

$$\omega^4-(\omega_c^2+\omega_p^2+\omega_2^2)\omega^2+[(1+\epsilon_2/2\epsilon_1)\omega_c^2+\omega_p^2]\omega_2^2=0 \quad (38)$$

where

$$\omega_2^2=2\epsilon_1\omega_p^2/(3\epsilon_2+2\epsilon_1) . \quad (39)$$

One of these modes, which is written to order $(\omega_c/\omega_p)^2$ as

$$\omega_{201}\simeq\omega_2+\tfrac{1}{6}\omega_c^2/\omega_2 , \quad (40)$$

is the ω_{201} mode of Furdyna *et al.*[35] The other mode,

$$\omega\simeq\omega_p+\tfrac{1}{3}\omega_c^2/\omega_p , \quad (41)$$

is the bulk magnetoplasmon of Goettig and Trzeciakowski[36] (GT). According to GT only the component of the oscillating magnetic field parallel to the dc applied magnetic field interacts with this mode, which arises from the $m=0$ magnetic dipole term. However, we find that this mode appears in the electric quadrupole and cross terms as well. To lowest order in ω_c/ω_p, the power absorbed due to the magnetic dipole term agrees with Eq. (57) of GT and the contribution of the remaining three terms is of higher order, which resolves the discrepancy.

For $m=\pm 1$, the condition for resonances is

$$\mathrm{Re}(3\epsilon_2+\epsilon_\pm+\epsilon_{zz})=0 . \quad (42)$$

For the lossless Drude plasma, the resonance frequencies are given by the real positive roots of

$$\omega^3\pm\omega_c\omega^2-\omega_2^2\left[\omega\pm\frac{\omega_c}{2}\right]=0 . \quad (43)$$

Note that the cyclotron frequency can be positive or negative depending on the sign of the carriers. This equation agrees with Eq. (23) of Furdyna *et al.*[35] for $l=2$. The expressions for the roots are quite complicated. For the low-field limit,

$$\omega_{2,\pm 1,1}\simeq\omega_{2\mp}\frac{\omega_c}{4}+\frac{5}{32}\frac{\omega_c^2}{\omega_2} \quad (44)$$

and

$$\omega_{2,-\mathrm{sgn}q,2}\simeq\frac{|\omega_c|}{2}\left[1-\frac{1}{4}\left[\frac{\omega_c}{\omega_2}\right]^2\right] \quad (45)$$

in agreement with Furdyna *et al.*[35] sgn$q$ denotes the sign of the carriers.

For $m=\pm 2$, resonances are located using

$$\mathrm{Re}(3\epsilon_2+2\epsilon_\pm)=0 . \quad (46)$$

For the lossless Drude plasma, this condition becomes

$$\omega^2\pm\omega_c\omega-\omega_2^2=0 . \quad (47)$$

The frequencies are

$$\omega=\mp\frac{\omega_c}{2}+\left[\left[\frac{\omega_c}{2}\right]^2+\omega_2^2\right]^{1/2} . \quad (48)$$

The power absorbed can also be calculated for the "lossless" plasma. It is related to the extinction cross section by

$$P=\sigma_{\mathrm{ext}}S \quad (49)$$

where S is the magnitude of the Poynting vector of the incident wave. Although our results do not appear similar at first glance they are identical to those obtained by Furdyna *et al.*,[35] who followed a quantum-mechanical approach: (1) Compute the modes of the system. (2) Write down the Hamiltonian. (3) Quantize it. (4) Use it to compute the power absorption by treating the interaction of the modes with a perturbing electromagnetic field. Our approach is classical. We take our results for the extinction cross section, plug in the dielectric tensor for the single-component Drude plasma, and take the lossless limit by letting the relaxation time become infinite. Use is made of the relation

$$\lim_{a\to 0}\frac{a}{x^2+a^2}=\pi\delta(x) . \quad (50)$$

Our results not only confirm the work of Furdyna *et al.*,[35] but are considerably more general because we can treat a sphere having any dielectric tensor consistent with Eq. (1). We may include phenomenological damping, multicomponent systems (which allow for many resonances, including types not seen for the simple example), optical phonons, and anisotropic carrier effective-mass tensors with the proper symmetry. The generality offers the possibility of comparison with data on real systems including powdered semiconductors (e.g., n-type InSb, n-type InAs),[2–9] electron-hole droplets (for specific orientations only),[10–22] and possibly the characterization of the new semiconductor "microdots."[47–51] Cyclotron resonance and magnetospectroscopy in general has been of use in the study of bulk and thin-film semiconductors as well as quantum wells, heterojunctions, and the two-dimensional electron gas.[52] If quantum dot structures take on some importance for new device structures, our expressions should be of use in the interpretation of magnetooptical data, particularly if the dots are spheres.

The behavior of the electric dipole extinction in an applied magnetic field in the long-wavelength limit is well known. What is new is the expression for the magnetic-dipole–electric-quadrupole extinction cross section. Experimentally, resonances have been observed for electric dipole excitations in several systems,[2–22] but there have been few reports of magnetic dipole excitations.[20] The magnetic-dipole–electric-quadrupole term is relatively

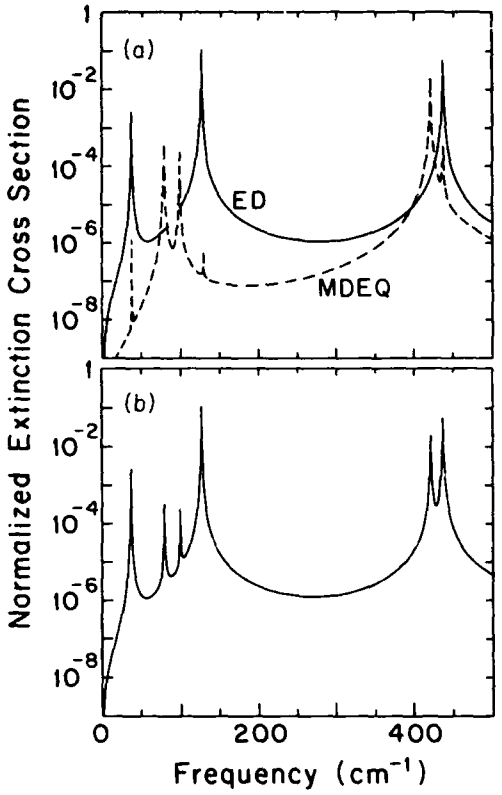

FIG. 1. Normalized extinction cross section for a small gyrotropic sphere. Parameters for a single-component Drude plasma are chosen to model a 1-μm-radius n-type InSb sphere in vacuum: $n=5\times10^{16}$ cm^{-3}, $m^*/m=0.014$, $1/\tau=0.5$ cm^{-1}, $\epsilon_l=18$, $\epsilon_2=1$. A 6-T magnetic field is applied in the z direction. The incident wave propagates in the x direction. (a) Electric dipole (ED), solid line, and magnetic-dipole–electric-quadrupole (MDEQ), dashed line, contributions. (b) Total extinction cross section in the long-wavelength limit. The ED term dominates, especially for the low-frequency (<150 cm^{-1}) group of resonances.

small and should be more difficult to observe, but the effect should be observable. Figure 1 shows the normalized extinction cross section $\sigma_{ext}/(\pi a^2)$, with parameters for the single-component Drude plasma chosen to model a 1-μm-radius sphere of n-type InSb in vacuum. Figure 1(a) shows the contributions of the electric dipole (ED) and magnetic-dipole–electric-quadrupole (MDEQ) terms separately. Figure 1(b) shows the total extinction cross section in the long-wavelength limit. The 6-T magnetic field is applied in the z direction. The incident electromagnetic wave propagates in the x direction. The MDEQ resonances are weaker by 2–3 orders of magnitude in the low-frequency multiplet below 150 cm^{-1}, and some of them overlap the ED resonances. The ED and MDEQ resonances are closer in magnitude for the group at high frequencies (>400 cm^{-1}). The strength of the MDEQ resonances relative to the ED resonances increases with particle size, but the applicability of the long-wavelength approximation becomes more questionable as well. The scattering rate was assigned a low value $[1/\tau(\text{cm}^{-1})]=0.5$ cm$^{-1}=1/[2\pi c\tau(\text{s})]$ to produce sharp resonances on the figure. If the resonances in actual materials are broader, MDEQ resonances will be more difficult to resolve and identify. For an experiment, it is important to have well-dispersed spherical particles with a controlled sharp size distribution. If the effective-mass tensors of the carriers are anisotropic, it is desirable that the particles be aligned.

IV. CONCLUSIONS

We have obtained the long-wavelength limit of the extinction cross section for a gyrotropic sphere from the general solution of Ford and Werner.[1] We applied the results to a lossless single-component Drude plasma sphere and obtained agreement with recent calculations by Furdyna *et al.*[35] and GT,[36] which were performed using a quasistatic approximation. Thus, our results resolve the discrepancy between these recent studies and the earlier, incorrect long-wavelength expressions. In addition, their generality permits potential applications to a number of actual materials.

ACKNOWLEDGMENT

This work was supported by the Office of Naval Research under Contract No. N00014-85-K-0808.

[1]G. W. Ford and S. A. Werner, Phys. Rev. B **18**, 6752 (1978).
[2]F. L. Galeener and J. K. Furdyna, Appl. Phys. Lett. **14**, 163 (1969).
[3]K. K. Chen, F. L. Galeener, and J. K. Furdyna, Appl. Phys. Lett. **16**, 387 (1970).
[4]F. L. Galeener and J. K. Furdyna, Phys. Rev. B **4**, 1853 (1971).
[5]F. L. Galeener, T. A. Evans, and J. K. Furdyna, Phys. Rev. Lett. **29**, 728 (1972); T. A. Evans, F. L. Galeener, and J. K. Furdyna, in *Proceedings of the XIth International Conference on the Physics of Semiconductors*, edited by M. Miasek *et al.* (Polish Scientific, Warsaw, 1972), p. 357.
[6]T. A. Evans and J. K. Furdyna, Phys. Rev. B **8**, 1461 (1973).
[7]J. R. Dixon, Jr., and J. K. Furdyna, Phys. Rev. B **18**, 6770 (1978).
[8]J. R. Dixon, Jr., and J. K. Furdyna, J. Appl. Phys. **51**, 3762 (1980).
[9]J. R. Dixon, Jr., and J. K. Furdyna, Solid State Commun. **35**, 195 (1980).
[10]T. Sanada, T. Ohyama, and E. Otsuka, Solid State Commun. **12**, 1201 (1973).
[11]V. N. Murzin, V. A. Zayats, and V. L. Kononenko, Fiz. Tverd. Tela (Leningrad) **15**, 3634 (1973) [Sov. Phys.—Solid State **15**, 2421 (1974)].
[12]R. S. Markiewicz, J. P. Wolfe, and C. D. Jeffries, Phys. Rev. Lett. **32**, 1357 (1974); **34**, 59(E) (1975).
[13]J. P. Wolfe, R. S. Markiewicz, C. D. Kittel, and C. D. Jeffries,

Phys. Rev. Lett. **34**, 275 (1975).
[14]K. Fujii and E. Otsuka, J. Phys. Soc. Jpn. **38**, 742 (1975).
[15]B. M. Ashkinadze and P. D. Altukhov, Fiz. Tverd. Tela (Leningrad) **17**, 1004 (1975) [Sov. Phys.—Solid State **17**, 643 (1975)].
[16]K. Muro and Y. Nisida, J. Phys. Soc. Jpn. **40**, 1069 (1976).
[17]V. I. Gavrilenko, V. L. Kononenko, T. S. Mandel'shtam, and V. N. Murzin, Pis'ma Zh. Eksp. Teor. Fiz. **23**, 702 (1976) [JETP Lett. **23**, 645 (1977)].
[18]V. L. Kononenko and V. N. Murzin, Pis'ma Zh. Eksp. Teor. Fiz. **24**, 590 (1976) [JETP Lett. **24**, 548 (1976)].
[19]V. I. Gavrilenko, V. L. Kononenko, T. S. Mandel'shtam, and V. N. Murzin, Dokl. Akad. Nauk. SSSR **232**, 802 (1977) [Sov. Phys.—Dokl. **22**, 82 (1977)].
[20]V. I. Gavrilenko, V. L. Kononenko, T. S. Mandel'shtam, V. N. Murzin, and S. A. Saunin, Pis'ma Zh. Eksp. Teor. Fiz. **26**, 102 (1977) [JETP Lett. **26**, 95 (1977)].
[21]P. G. Baranov, Yu. P. Veschunov, R. A. Zhitnikov, N. G. Romanov, and Yu. G. Shreter, Pis'ma Zh. Eksp. Teor. Fiz. **26**, 369 (1977) [JETP Lett. **26**, 249 (1977)].
[22]H. Nakata, K. Fujii, and E. Otsuka, J. Phys. Soc. Jpn. **45**, 537 (1978).
[23]R. S. Markiewicz and T. Timusk, in *Electron-Hole Droplets in Semiconductors*, edited by C. D. Jeffries and L. V. Keldysh (North-Holland, New York, 1983), pp. 543–618.
[24]G. Mie, Ann. Phys. (Leipzig) **25**, 377 (1908).
[25]P. Debye, Ann. Phys. (Leipzig) **30**, 57 (1909).
[26]H. C. van de Hulst, *Light Scattering by Small Particles* (Dover, New York, 1981), p. 270.
[27]C. F. Bohren and D. R. Huffman, *Absorption and Scattering of Light by Small Particles* (Wiley, New York, 1983), pp. 130–135.
[28]W. L. Bragg and A. B. Pippard, Acta Crystallogr. **6**, 865 (1953).
[29]C. Jones, Phys. Rev. **68**, 93 (1945); **68**, 213 (1945).
[30]J. C. M. Garnett, Philos. Trans. R. Soc. London **203**, 385 (1904); **205**, 237 (1906).
[31]D. A. G. Bruggeman, Ann. Phys. (Leipzig) **24**, 636 (1935).
[32]G. W. Ford, J. K. Furdyna, and S. A. Werner, Phys. Rev. B **12**, 1452 (1975).
[33]J. R. Dixon, Jr., and J. K. Furdyna, Phys. Rev. B **19**, 4167 (1979).
[34]R. S. Markiewicz, Phys. Rev. B **18**, 4260 (1978).
[35]J. K. Furdyna, S. Goettig, J. Mycielski, and W. Trzeciakowski, Phys. Rev. B **31**, 7714 (1985).
[36]S. Goettig and W. Trzeciakowski, Phys. Rev. B **31**, 7726 (1985).
[37]C. J. Crowell and R. H. Ritchie, Phys. Rev. **172**, 436 (1968).
[38]J. C. Ashley, T. L. Ferrell, and R. H. Ritchie, Phys. Rev. B **10**, 554 (1974).
[39]V. L. Kononenko and V. N. Murzin, Zh. Eksp. Teor. Fiz. **75**, 124 (1978) [Sov. Phys.—JETP **48**, 61 (1979)].
[40]V. L. Kononenko, Fiz. Tverd. Tela (Leningrad) **17**, 3264 (1975) [Sov. Phys.—Solid State **17**, 2146 (1976)].
[41]A. R. Edmonds, *Angular Momentum in Quantum Mechanics* (Princeton University Press, Princeton, NJ, 1951).
[42]J. M. Blatt and V. F. Weiskopf, *Theoretical Nuclear Physics* (Wiley, New York, 1952), Appendix B.
[43]G. W. Ford and S. A. Werner, Phys. Rev. B **8**, 3702 (1973), Appendix B.
[44]*Handbook of Mathematical Functions*, edited by M. Abramowitz and I. A. Stegun (U.S. GPO, Washington, D.C., 1964).
[45]G. Dresselhaus, A. F. Kip, and C. Kittel, Phys. Rev. **98**, 368 (1955); **100**, 618 (1955).
[46]F. L. Galeener, Phys. Rev. Lett. **22**, 1292 (1969).
[47]M. A. Reed, R. T. Bate, K. Bradshaw, W. M. Duncan, W. R. Frensley, J. W. Lee, and H. D. Shih, J. Vac. Sci. Technol. B **4**, 358 (1969).
[48]K. Kash, A. Scherer, J. M. Worlock, H. G. Craighead, and M. C. Tamargo, Appl. Phys. Lett. **49**, 1043 (1986).
[49]J. Cibert, P. M. Petroff, G. J. Dolan, S. J. Pearton, A. C. Gossard, and J. H. English, Appl. Phys. Lett. **49**, 1275 (1986).
[50]H. Temkin, G. J. Dolan, M. B. Parrish, and S. N. G. Chu, Appl. Phys. Lett. **50**, 413 (1987).
[51]R. L. Kubena, R. J. Joya, J. W. Ward, H. L. Garvin, F. P. Stratton, and R. G. Brault, Appl. Phys. Lett. **50**, 1589 (1987).
[52]T. Ando, A. B. Fowler, and F. Stern, Rev. Mod. Phys. **54**, 437 (1982), and references therein.

Send correspondence to :
R.E. Sherriff
Department of Physics and Astronomy
100 Allen Hall
University of Pittsburgh
Pittsburgh, Pa. 15260 USA
(412) 624-9084
keywords: Far infrared, Absorption, Small Metal Particles, Bismuth

Far Infrared Absorption by Small Bismuth Particles

Running Title: FIR Absorption by Small Bismuth Particles

R.E. Sherriff and R.P. Devaty
Department of Physics and Astronomy
100 Allen Hall
University of Pittsburgh
Pittsburgh, Pa 15260 USA

Abstract

We have observed low frequency ($< 50\ cm^{-1}$) magnetic field dependent resonances and higher frequency resonances at zero field in the far infrared (FIR) absorption of small bismuth particles. A model based on the quasistatic approximation shows both good agreement with previous measurements of resonance frequencies vs. field and qualitative agreement with our data. Additional work is required to quantify the comparison.

Introduction

Bismuth is often used as a model system for solid state plasmas because many of its important energies (E_F, $\hbar\omega_p$, etc.) are conveniently close together in the FIR. The properties of Bi make it especially interesting for FIR magneto-optical studies because the interaction of the cyclotron-like resonances with the plasma modes can be seen using currently achieveable fields. The low carrier density also implies a large Kubo gap [1], enhancing the possibility of seeing quantum size effects (QSE) or metal-insulator transitions.

One of the earliest studies of small Bi particles was carried out by Chin and Sievers [2]. Motivated by the idea that free Bi particles appeared to align the bisectrix axis along the applied magnetic field [3], they performed FIR transmission measurements on free-standing Bi particles and

found three field dependent resonances. No successful explanation of these lines was given. We have developed a model using bulk Bi parameters that agrees well with the data. The model also predicts additional resonances in and above the frequency range covered by Chin. To search for these additional resonances, we investigated the FIR absorption of small Bi particles both at low frequencies in a magnetic field and at higher frequencies at zero field.

Theory

Chin's data (Figure 1) can be successfully modelled by treating the Bi particles as small spheres with an anisotropic dielectric tensor $\mathbf{\varepsilon}$. The quasistatic boundary value problem [4] is solved to find α (the absorption coefficient) :

$$\alpha(\omega) = \frac{9}{2} f\sqrt{\epsilon_o}\left(\frac{\omega}{c}\right) \mathrm{Im}\left\{\hat{E}^* \cdot B^{-1} \cdot \hat{E}\right\} + \frac{1}{5} f\, d^2 \sqrt{\epsilon_o}\left(\frac{\omega}{c}\right)^3 \mathrm{Im}\left\{\hat{B}^* \cdot \overline{\varepsilon^{-1}}^{-1} \cdot \hat{B}\right\} \qquad (1)$$

where ω is the angular frequency, ϵ_o the dielectric constant of the surrounding medium, ε the dielectric tensor of the sphere, d the particle diameter, and f the volume fraction of Bi. The tensors in the expression are given by $B = 1 + 2\epsilon_o \varepsilon^{-1}$ and $\overline{\varepsilon^{-1}} = \mathrm{Tr}(\varepsilon^{-1})1 - (\varepsilon^{-1})^T$.

To get ε for a small Bi sphere, we use an anisotropic Drude model with bulk parameters [5] *for the four carriers :*

$$\varepsilon = \varepsilon_L - \frac{4\pi q^2}{\omega\bar{\omega}} \sum_{j=1}^{4} n_j (m_j^*)^{-1} \qquad (2)$$

Here n_j is the number density and m_j^* the effective mass tensor for the j^{th} carrier. ε_L is a frequency independent tensor [5], q the electronic charge, and $\bar{\omega} = \omega + \frac{i}{\tau}$. [Note: The magnetic dipole term (2^{nd} term in Eq. 1) is incorrect due to neglect of the electric quadrupole term [6]. However, the large value of ε_L for Bi makes the corrections small.]

Figure 1 compares the Chin data with the theory. The data agree remarkably well with three of the theoretical curves, allowing us to identify two of the curves as electric dipole resonances, and one as magnetic dipole. The model, however, also predicts a large number of lines that aren't seen in these data as well as resonances that should exist at higher frequencies, even with H=0.

Experiment

We used two approaches to test the model. First we looked for additional low frequency field dependent resonances in free-standing powders. The powders themselves limited the upper cutoff frequency to around 50 cm^{-1}. To search for higher frequency resonances we used pressed pellets of Bi in paraffin. This enabled us to use low volume fractions of Bi and raise the cut-off frequency.

The Bi particles were prepared by inert gas evaporation in Ar [7]. Size distributions were obtained from transmission electron micrographs. Electron diffraction patterns indicated that the particles were crystalline.

Samples of free-standing powders were made by spreading a thin, approximately uniform layer of powder onto a Mylar sheet and then sandwiching it with another layer of Mylar to keep it in place during sample insertion.

To prepare pressed pellets, the Bi powder was first mixed with paraffin powder and manually shaken. The paraffin was then melted and the suspension of Bi particles was stirred. After resolidifying, the sample was repeatedly ground in a freezer mill at 77°K and then pressed into half inch diameter pellets. The grinding/pressing cycle was repeated 3-4 times.

The transmission of the free-standing powder was measured in the Faraday geometry for various magnetic fields using a Michelson interferometer over the range 10 - 50 cm^{-1}. For the pressed pellets, we measured the FIR absorption coefficient, again with a Michelson but over the range 30 - 300 cm^{-1}.

The results of our study on a free-standing Bi powder appear in Figure 2 as ratios of spectra with field to spectra without field. Arrows indicate the locations of possible resonances, but many of the identifications must be considered tentative because of their small size (slightly larger than noise in the spectra). Even discounting some of the smaller, less trustworthy resonances, the data still show an abundance of field dependent absorption peaks providing at least qualitative support for our model.

Quantitative comparison on the other hand is difficult. In addition to the small size of many resonances, interpretation of the data is further complicated by the changing size of the peaks as they move upward in frequency. This makes it difficult to unambiguously trace the field dependence of each resonance from curve to curve, especially in regions where the magnetic field sampling interval is more than 1kG. Further confusion results from the low transmission level of the samples which both decreases SNR (raising doubts about the smaller resonances) and limits the frequency range over which resonances can be tracked. A direct quantitative evaluation of the model beyond the agreement with Chin's data must wait until additional experiments in progress are completed.

It is possible however to obtain support for our model from the pressed pellet data shown in Figure 3. The absorption coefficient at zero field shows a resonance within 7% of the predicted location for the zero field combined dipole peak for randomly oriented particles. The theory predicts two peaks but it is possible that the resonances are too broad to be resolved.

Conclusions

We have developed a model for the far infrared absorption of small Bi particles that agrees

with the data of Chin [2]. Our own experimental evidence of a large number of field dependent resonances below 50 cm^{-1} and a strong resonance around 180 cm^{-1} at zero field also suggests at least a qualitative agreement with the model. A direct quantitative comparison awaits the collection of more data.

Acknowledgement

This work was supported by ONR Contract #N00014-85-K-0808.

References

[1] R. Kubo, J. Phys. Soc. Jpn. 17 (1962) 975

[2] A.K. Chin, Ph.D. Thesis, Cornell University (MSC Report #2823), USA (1977) .

[3] J. Feder and D.S. McLachlan, Phys. Lett. 29A (1969) 431 .

[4] R.S. Markiewicz, Phys. Rev. B 18 (1978) 4260 .

[5] R.L. Blewitt and A.J. Sievers, J. Low Temp. Phys. 13 (1973) 617 .

[6] R.P. Devaty, to be published in Phys. Rev. B15 .

[7] C.G. Granqvist and R.A. Buhrman, J. Appl. Phys. 47 (1976) 2200 .

Figure Captions

Fig. 1. Field dependent resonances for 4000Å diameter free standing bismuth particles. The symbols show data while the lines represent calculations based on our model. Solid lines indicate magnetic dipole curves while dashed lines are electric dipole.

Fig. 2. Relative transmission spectra of 5000Å diameter free standing bismuth particles for five different values of the magnetic field. The dashed lines are at the 100% level for each curve. All the curves are plotted with the same vertical scale. Arrows indicate possible locations of resonance peaks.

Fig. 3. FIR absorption coefficient for 1 μm bismuth particles in paraffin. The absorption coefficient for paraffin is shown for comparison.

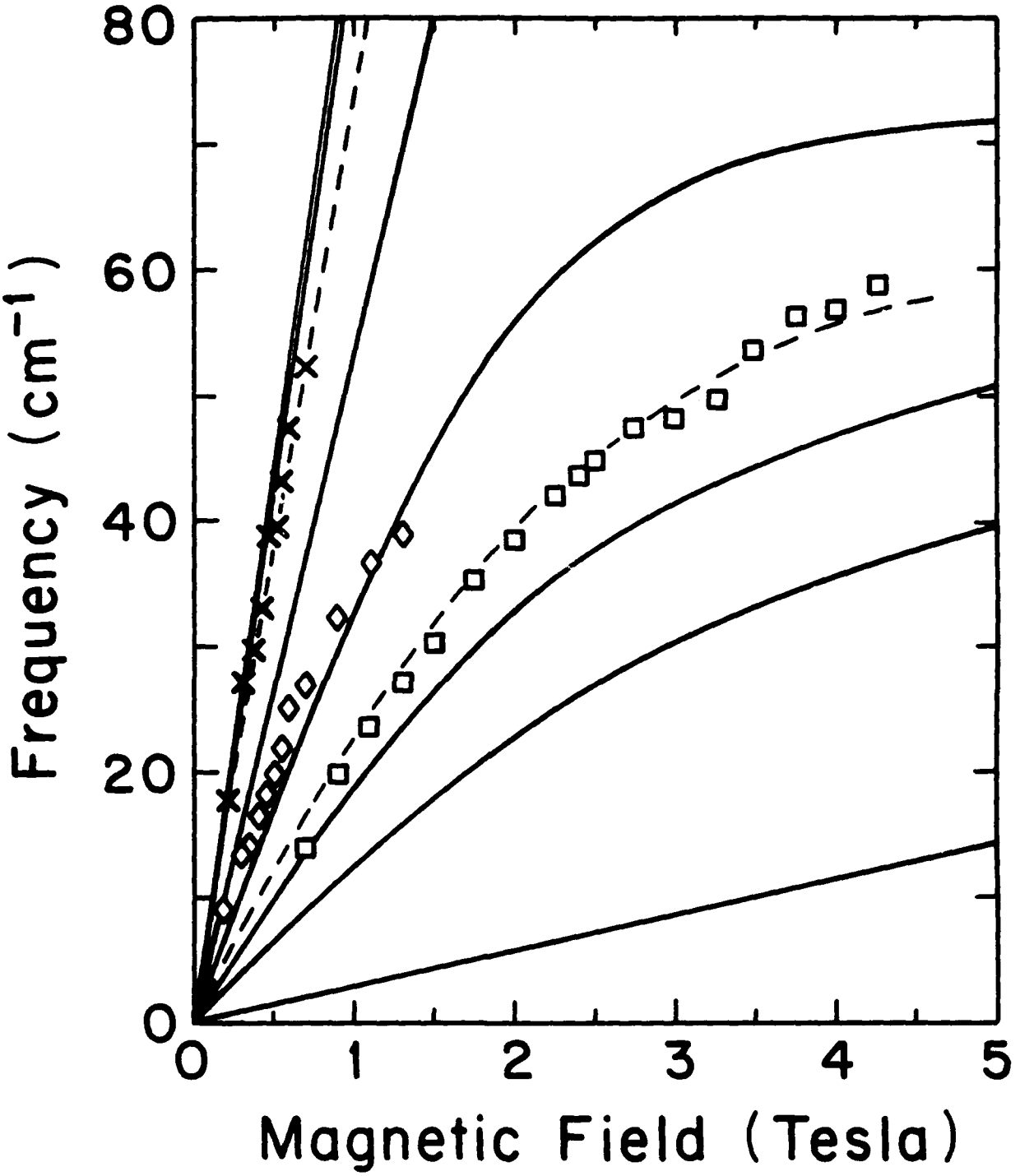
80
60
40
20
0
0
1
2
3
4
5
Frequency (cm^{-1})
Magnetic Field (Tesla)

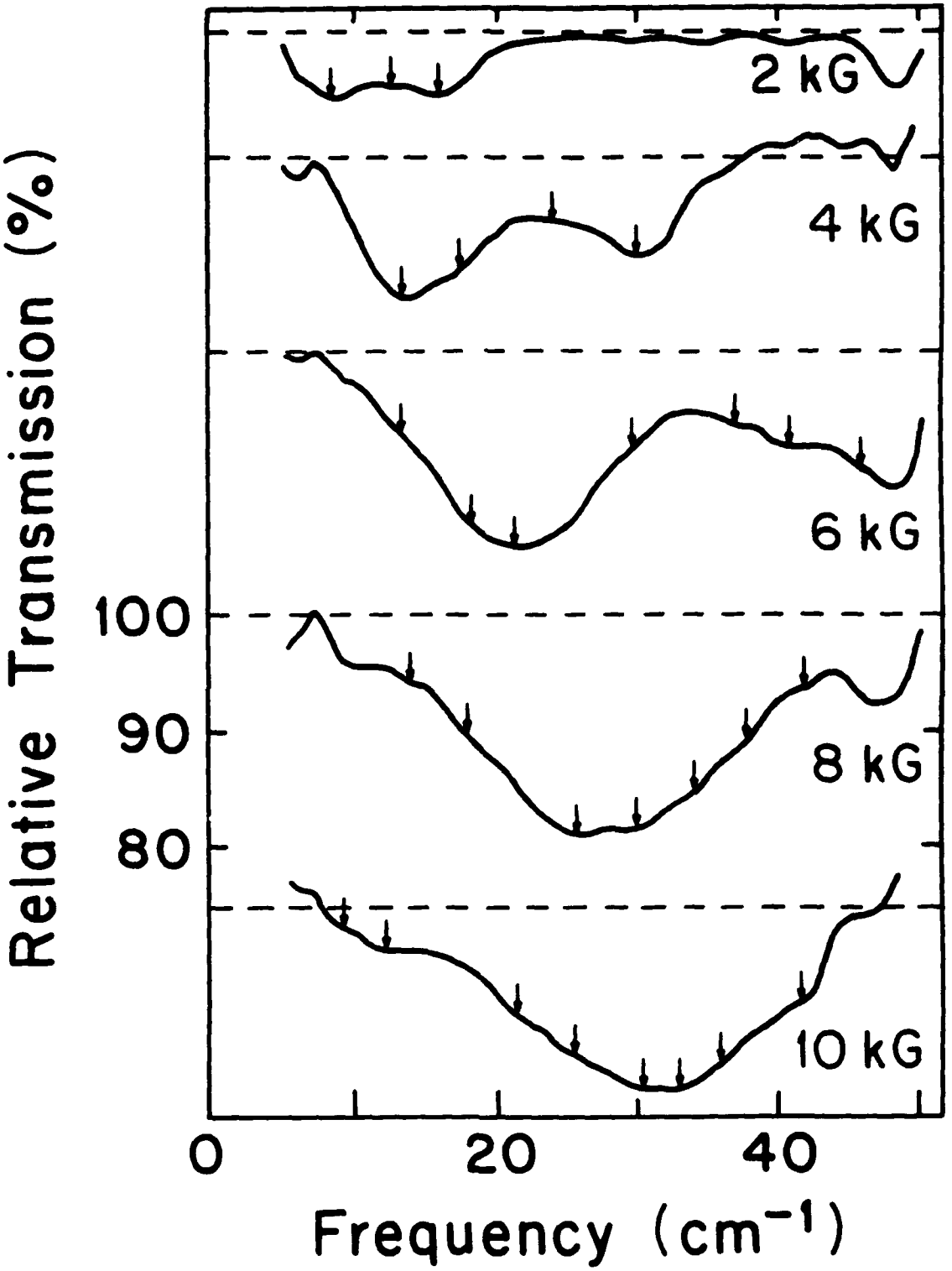
2 kG
4 kG
6 kG
8 kG
10 kG
100
90
80
Relative Transmission (%)
0
20
40
Frequency (cm⁻¹)

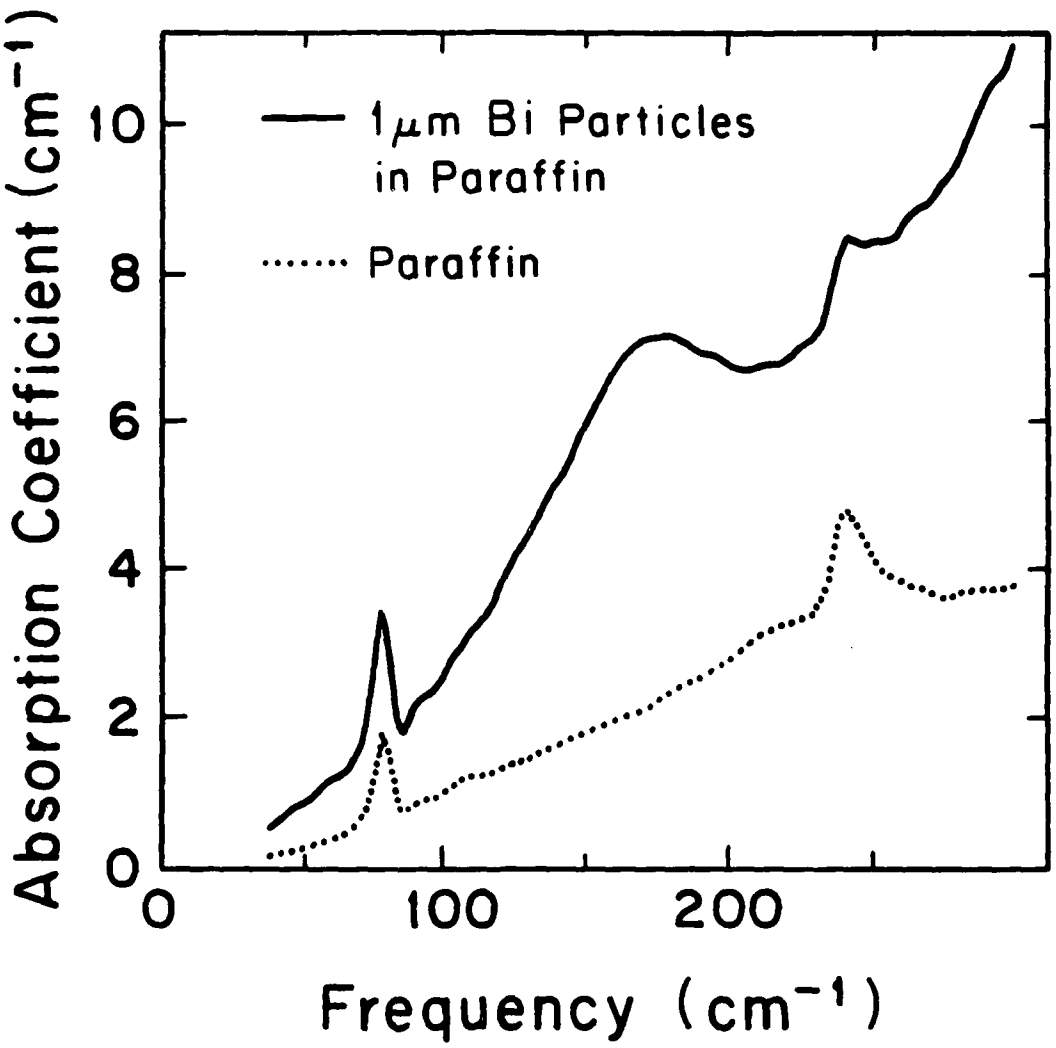
Absorption Coefficient (cm⁻¹)
0
2
4
6
8
10
0
100
200
Frequency (cm⁻¹)
1μm Bi Particles in Paraffin
Paraffin

Send correspondence to:
Robert P. Devaty
Department of Physics and Astronomy
100 Allen Hall, University of Pittsburgh
Pittsburgh, PA 15260, USA
Phone: (412) 624-9009

Keywords: absorption, far infrared, quantum size effects, metal particles

August 18, 1988

THE SECOND INTERNATIONAL CONFERENCE ON ELECTRICAL TRANSPORT AND OPTICAL PROPERTIES OF INHOMOGENEOUS MEDIA

INVITED PAPER

INFRARED ABSORPTION OF INHOMOGENEOUS MEDIA WITH METALLIC INCLUSIONS

Running Title: Infrared Absorption of Inhomogeneous Media

Robert P. Devaty
Department of Physics and Astronomy
100 Allen Hall
University of Pittsburgh
Pittsburgh, PA, 15260

ABSTRACT

The absorption of far infrared radiation by small metal particles and metal-insulator composite materials is reviewed. The possibility of observing quantum size effects is examined. Recent experimental and theoretical progress in understanding the anomalous enhancement of the far infrared absorption coefficient is discussed.

I. Introduction

This paper briefly reviews the present understanding of the interaction of far infrared (FIR) radiation with small metal particles and metal-insulator composite materials. The important issues of quantum size effects (QSE), the anomalous enhancement of the far infrared absorption coefficient, and other recent activity are discussed. This paper is an update to several more detailed reviews [1-4] of this topic.

II. Quantum Size Effects

Interest in the far infrared absorption by small metal particles was initially motivated at least in part by the possibility of observing transitions between discrete levels. The effects of confinement on the energy levels of the conduction electrons in a particle can be described by quantum box models, as first discussed by Fröhlich [5] and later refined by others [6-10]. The levels calculated in these models tend to have a high degree of degeneracy due to the assumed symmetry of the particle (usually a cube or sphere). Details in the optical structure predicted by these models are not presently observable due to imperfections in the shapes of particles, surface roughness, and the inevitable distribution of sizes.

Kubo [11] introduced a statistical approach to QSE's in ultrafine metal particles. He estimated the level spacing at the Fermi energy E_F of a particle by inverting the density of electron states at E_F for a given spin to obtain the "Kubo gap" $\delta = 4E_F/3nV$, where n is the density of free carriers and V the volume of the particle. Using free electron values, δ is on the order of $10cm^{-1}$ (1 meV) for typical metals (Al, Ag, Au, Cu, ...). An exceptionally large δ is predicted for Bi particles [12].

Gor'kov and Eliashberg (GE) [13] asserted that Kubo's use of the Poisson distribution to describe the level statistics neglects correlations between the levels. According to GE, the randomness of the level distribution in an ensemble of metal particles introduced by surface roughness is described by the statistical theory of levels (random matrix theory) originally developed by Wigner [14], Dyson and Mehta [15], and others for applications in nuclear physics. After corrections for a number of errors in the original paper [16-18], the GE model predicts oscillations in the frequency dependence of the FIR absorption coefficient superimposed on a quadratic background. When account is taken of the particle size distribution present in actual samples, the signatures of QSE's disappear [18]. At present no evidence has been obtained for QSE's in small metal particles by a far infrared experiment. Thus, theory and experiment are presently in agreement, but a rigorous test of the theory requires the ability to manufacture particles with a very sharp size distribution.

Devaty and Sievers [19] reexamined the possibility of observing QSE's by absorption spectroscopy and found reduced absorption for frequencies below the mean Kubo gap. The effect is weak, but persists even in the presence of a size distribution.

An anomalously low microwave conductivity recently observed [20] for small indium particles dispersed in oil has been interpreted as evidence for a QSE [21] using the GE model.

Shklovskii [22] discussed a modification to GE's argument based on electron-electron interactions and concluded that the frequency dependence of the FIR absorption coefficient predicted by GE must be reduced by a factor of $\hbar\omega/\delta$.

Random matrix theory has been an active area of research recently [23]. Efetov [24] derived the two-level correlation functions for Dyson's three circular ensembles using the mathematics of supersymmetry. Several groups have questioned the assumptions underlying the GE model [25-28], particularly whether randomness introduced by boundary conditions can be described by random matrices. The issue appears to be unresolved at this time.

III. The Anomalous Far Infrared Absorption

Most measurements of the far infrared absorption coefficient of small metal particles imbedded in an insulating host have been performed on samples having a low metallic volume fraction f. In the limit of low f, long wavelength, and assuming that the particles are randomly dispersed, the predictions of effective medium theories reduce to a simple expression which can also be obtained from the Mie-Debye solution for a single sphere. For a Drude metal particle imbedded in a nonabsorbing host, with the bulk relaxation time replaced by v_F/a (v_F = Fermi velocity, a=particle radius), the FIR absorption coefficient α reduces to the sum of electric (ED) and magnetic (MD) dipole terms with the properties: 1) quadratic frequency dependence, 2) size dependence: $\alpha_{ED} \sim a^{-1}$ and $\alpha_{MD} \sim a^3$, 3) For a typical metal, say Al, the MD term dominates for diameters greater than $50\mathring{A}$.

An enhancement of one to four orders of magnitude in the FIR absorption coefficient of small metal particles and metal-insulator composites with respect to theoretical predictions was discovered by Tanner et al. [29] and subsequently characterized [30-33]. The samples under study were typically particles prepared by inert gas evaporation [34], sometimes in the presence of O_2 to produce an oxide coating, and dispersed in an alkali halide host by repeated grinding and pressing into pellets. Free-standing particles (smokes) were also examined. The principal results are the ubiquity of the enhancement (observed for Al, Ag, Au, Cu, Pd, Sn, and Pt), an approximately quadratic frequency dependence, and a linear dependence on f for small f (with the exception of Al[33]). In addition to the enhancement, the far infrared properties of superconducting particles showed anomalous behavior in the region of the gap [35].

A number of mechanisms were proposed in attempts to explain the anomalous absorption. Mechanisms intrinsic to isolated particles include vibrations [36-37], eddy currents and nonlocal effects [38-40], particle size distributions [41], Coulomb effects [42], and quantum size effects [43]. Mechanisms for enhancements induced by clustering include

oxide-coated clusters [44,45], eddy current losses [46], and geometrical effects (shape, close approach of spheres) [46]. These mechanisms do not explain the enhancement in a satisfactory manner, either because the experimental result is larger than theory or because the proposed explanation is too specific to cover all the experiments.

An experimental breakthrough occurred with the realization of the importance of well-characterized samples with controllable properties to distinguish among proposed mechanisms. Devaty and Sievers [47] developed a novel composite material, $\sim 100\mathring{A}$ Ag particles supported in gelatin, that could be sectioned with an ultramicrotome for examination by transmission electron microscopy as well as pressed into pellets for FIR measurements. Samples could be prepared with the particles well-dispersed or deliberately agglomerated. Studies of this material provided evidence for the important role of clustering to the enhancement. Bounds were placed on the magnitude of the enhancement for dispersed particles (Absorption by the gelatin dominated absorption by the particles). Deliberate clustering produced an increase in absorption.

Additional experiments provided further important clues. Curtin et al. [48] showed that a heat treatment (melting the particles) eliminated the anomalous behavior of superconducting Sn particles near the gap. This experiment motivated the models of Curtin and Ashcroft [49], which provide an explanation for the enhancement. Lee et al. [50] introduced a new host, DLX-6000, a teflon-like material, which can be ultramicrotomed for electron microscopy but, unlike gelatin, is a weak FIR absorber. They studied fairly large Ag particles imbedded in teflon and were able to obtain agreement with theory for dispersed particles and demonstrated enhanced absorption for a clumped sample.

The results of these experiments directed theorists to focus on clustering as a mechanism for enhanced FIR absorption. Curtin and Ashcroft [49] introduced three different models. In the fused cluster model, a dense cluster is modeled as a metallic sphere with a scattering time determined by the radius of an individual particle. The short relaxation time leads to enhanced eddy current (MD) absorption. The cluster percolation model treats a cluster as a sphere made up of an effective medium. The sample is modeled as a dilute mixture of clusters which make up a second effective medium. Enhanced absorption occurs for clusters with f near the dc percolation threshold f_c; i.e., there is a resonance in f. The enhanced ED absorption is caused by the tortuous, poorly conducting clusters near f_c. Although Curtin and Ashcroft modeled their cluster using a treatment based on the real space renormalization group, any effective medium theory with a percolation threshold should do the job, at least qualitatively. Perhaps the simplest approach is to model the clusters using the Bruggeman model [51] and use the Maxwell-Garnett model [52] to average over the clusters. The third model, the cluster-tunnel junction model, applies to closely spaced oxide-coated particles in clusters.The absorption mechanism is photon-induced electron transfer. Hui and Stroud [53] modeled a cluster using a self-similar effective medium theory [54] and examined a possible role for tenuous fractal clusters in the enhanced absorption. Niklasson et al. [55] also examined fractal clusters. Claro and Fuchs [56] modeled clusters of particles by introducing a distribution of effective depolarization factors. They obtained an enhancement of 3-4 orders of magnitude in the FIR ED absorption.

In addition to clustering, recent theoretical work has considered other mechanisms including surface phonons [57], electron-phonon coupling [58], diffuse surface scattering [59], relaxation time effects [60], and quantum size effects [61].

Recent experimental work in the far infrared has focussed on new issues. Previous studies at low temperature ($T < 20K$) showed no evidence for temperature dependence in α. Noh et al. [62] have measured the temperature dependence of α for a Ag-teflon composite from room temperature down to liquid He temperatures and observed a small ($\sim$ 10%) effect. They found satisfactory agreement with a model which included the effects of oxide coats, particle size distribution, and modification of the electronic relaxation time due to impurities within the particles. Lee et al. [50, 63] showed that oxide coatings lead to enhanced absorption in the mid and far infrared. Sherriff and Devaty [12] have studied the unusual FIR properties of Bi particles. Kuroda et al. [64] have measured FIR absorption by small particles of the high-T_c superconductor $YBa_2Cu_3O_{6.74}$. Sievers' group [65] applied the Bruggeman model [51] to FIR data on sintered pellets of high-T_c superconductors and related compounds.

The role of clustering in the anomalous enhancement of the FIR absorption coefficient appears to be understood. However, there are some unresolved issues. The dependence of α on particle size has not been systematically studied. The inevitable size distributions make such a study difficult, but theoretical predictions should be tested experimentally. In addition, there have been few FIR studies of metal-insulator composite materials over a large or complete range of composition [66]. Such studies, which might focus on the region of dc percolation, would test effective medium theories and extend similar studies in the ir-vis-uv into a new spectral region.

Acknowledgement

This work was supported by ONR Contract N00014-85-K-0808.

References

[1] G. L. Carr, S. Perkowitz, and D. B. Tanner, in: Infrared and Millimeter Waves, Vol. 15, K. J. Button, ed. (Academic Press, Orlando, 1984).

[2] W. P. Halperin, Rev. Mod. Phys. 58 (1986) 533.

[3] J.A.A.J. Perenboom, P. Wyder, and F. Meier, Phys. Repts. 78 (1981) 173.

[4] H.P. Baltes and E. Simanek, in: Aerosol Microphysics II, Topics in Current Physics, Vol. 29, W.H. Marlow, ed. (Springer-Verlag, Berlin, 1981), p. 7.

[5] H. Fröhlich, Physica (Utrecht) 4 (1937) 406.

[6] L. Genzel, T.P. Martin, and U. Kreibig, Z. Phys. B21 (1975) 339.

[7] M. Cini and P. Ascarelli, J. Phys. F: Metal Physics 4 (1974) 1998.

[8] M. Cini, J. Opt. Soc. Am. 71 (1981) 386.

[9] D.M. Wood and N.W. Ashcroft, Phys. Rev. B25 (1982) 6255.

[10] L. Genzel and U. Kreibig, Z. Phys. B37 (1980) 93.

[11] R. Kubo, J. Phys. Soc. Jpn. 17 (1962) 975.

[12] R.E. Sherriff and R.P. Devaty, Physica A, this issue.

[13] L.P. Gor'kov and G.M. Eliashberg, Sov. Phys.-JETP 21 (1965) 940.

[14] E.P. Wigner, Ann. Math. 53 (1951) 35; 62 (1955) 548.
[15] F.J. Dyson, J. Math. Phys. 3 (1962) 140; 3 (1962) 166; M.L. Mehta and F. J. Dyson, J. Math. Phys. 4 (1963) 713.
[16] S. Strassler, M.J. Rice, and P. Wyder, Phys. Rev. B6 (1972) 2575.
[17] A.A. Lushnikov and A.J. Simonov, Phys. Lett. A44 (1973) 45.
[18] R.P. Devaty and A.J. Sievers, Phys. Rev. B22 (1980) 2123.
[19] R.P. Devaty and A.J. Sievers, Phys. Rev. B32 (1985) 1951.
[20] P. Marquardt, L. Borngen, G. Nimtz, H. Gleiter, and J. Zhu, Phys. Lett. A114 (1986) 39.
[21] P. Marquardt, Phys. Lett. A123 (1987) 365.
[22] B.I. Shklovskii, JETP Lett. 36 (1983) 352.
[23] T.A. Brody, J. Flores, J. B. French, P.A. Mello, A. Pandy, and S.S.M. Wong, Rev. Mod. Phys. 53 (1981) 385.
[24] K.B. Efetov, Sov. Phys.-JETP 56 (1983) 467; J. Phys. C: Solid State Phys. 15 (1982) L909; Adv. Phys. 32 (1983) 53.
[25] J. Barojas, E. Cota, E. Blaisten-Barojas, J. Flores, and P.A. Mello, Ann. Phys. (New York) 107 (1977) 95; J. Phys. (Paris) Colloque 38 (1977) C2-129.
[26] J. Barojas, E. Blaisten-Barojas, and J. Flores, Phys. Lett. A69 (1978) 142.
[27] J.F. Tavel, K.F. Ratcliff, and N. Rosenzweig, Phys. Lett. A73 (1979) 353.
[28] S. Tanaka and S. Sugano, Phys. Rev. B34 (1986) 740; B34 (1986) 6880.
[29] D.B. Tanner, A.J. Sievers, and R.A. Buhrman, Phys. Rev. B11 (1975) 1330.
[30] C.G. Granqvist, R.A. Buhrman, J. Wyns, and A.J. Sievers, Phys. Rev. Lett. 37 (1976) 625.
[31] D.P. Pramanik, M.S. Thesis, Cornell University (1978).
[32] N.E. Russell, J.C. Garland, and D.B. Tanner, Phys. Rev. B23 (1981) 632.
[33] G.L. Carr, R.L. Henry, N.E. Russell, J.C. Garland, and D.B. Tanner, Phys. Rev. B 24 (1981) 777.
[34] C.G. Granqvist and R.A. Buhrman, J. Appl. Phys. 47 (1976) 2200.
[35] G.L. Carr, J.C. Garland, and D.B. Tanner, Phys. Rev. Lett. 50 (1983) 1607.
[36] A.J. Glick, and E.D. Yorke, Phys. Rev. B18 (1978) 2490.
[37] E. Simanek, Solid State Commun. 37 (1981) 97.
[38] H.J. Trodahl, Phys. Rev. B19 (1979) 1316; J. Phys. C: Solid State Phys. 15 (1982) 7245.
[39] A.G. Mal'shukov, Sov. Phys. -JETP 58 (1983) 409.
[40] P. Apell, Physica Scripta 29 (1984) 146.
[41] P. Chylek, D. Boice, and R.G. Pinnick, Phys. Rev. B27 (1983) 5107. See also D.B. Tanner, Phys. Rev. B30 (1984) 1042; P. Chylek and V. Srivastava, Phys. Rev. B30 (1984) 992.

[42] A.A. Lushnikov, V.V. Maksimenko, and A.J. Simonov, in: Electromagnetic Surface Modes, J. Boardman, ed. (Wiley, New York, 1982), Chp. 8; Sov. Phys. Solid State 20 (1978) 292; V.V. Maksimenko, A.J. Simonov, and A.A. Lushnikov, Phys. Stat. Sol. (b) 83 (1977) 377; A.A. Lushnikov and A.J. Simonov, Phys. Lett. 44A (1973) 45.

[43] C.G. Granqvist, Z. Phys. B30 (1978) 29.

[44] E. Simanek, Phys. Rev. Lett. 38 (1977) 1161.

[45] R. Ruppin, Phys. Rev. B19 (1979) 1318.

[46] P.N. Sen and D.B. Tanner, Phys. Rev. B26 (1982) 3582.

[47] R.P. Devaty and A.J. Sievers, Phys. Rev. Lett. 52 (1984) 1344.

[48] W.A. Curtin, R.C. Spitzer, N.W. Ashcroft, and A.J. Sievers, Phys. Rev. Lett. 54 (1985) 1071.

[49] W.A. Curtin and N.W. Ashcroft, Phys. Rev. B31 (1985) 3287.

[50] S.-I. Lee, T.W. Noh, K. Cummings, and J.R. Gaines, Phys. Rev. Lett. 54 (1985) 1626.

[51] D.A.G. Bruggeman, Ann. Phys. (Leipzig) 24 (1935) 636.

[52] J.C.M. Garnett, Phil. Trans. R. Soc. London 203 (1904) 385; 205 (1906) 237.

[53] P.M. Hui and D. Stroud, Phys. Rev. B33 (1986) 2163.

[54] P.N. Sen, C. Scala, and M.H. Cohen, Geophys. 46 (1981) 781.

[55] G.A. Niklasson, S. Yatsuya, and C.G. Granqvist, Solid State Commun. 59 (1986) 579.

[56] F. Claro and R. Fuchs, Phys. Rev. B33 (1986) 7956.

[57] R. Monreal, J. Giraldo, F. Flores, and P. Apell, Solid State Commun. 54 (1985) 661.

[58] X.M. Hua and J.I. Gersten, Phys. Rev. B31 (1985) 855.

[59] P. de Andres, R. Monreal, and F. Flores, Phys. Rev. B34 (1986) 2886.

[60] P. de Andres, R. Monreal, and F. Flores, Phys. Rev. B34 (1986) 7365.

[61] R. Monreal, P. de Andres, and F. Flores, J. Phys. C: Solid State Phys. 18 (1985) 4951.

[62] T.W. Noh, S.-I, Lee, and J.R. Gaines, Phys. Rev. B33 (1986) 1401; T.W. Noh, S.-I. Lee, Y. Song, and J.R. Gaines, Phys. Rev. B34 (1986) 2882.

[63] S.-I. Lee, T.W.Noh, and J.R. Gaines, Phys. Rev. B32 (1985) 3580; S.-I. Lee, T.W. Noh, J. Golben, and J.R. Gaines, Phys. Rev. B33 (1986) 5844.

[64] N. Kuroda, F. Chida, Y. Sasaki, Y. Nishina, M. Kikuchi, A. Tokiwa, and Y. Syono, J. Phys. Soc. Jpn. 56 (1987) 3797.

[65] P.E. Sulewski, T.W. Noh, J.T. McWhirter, and A.J. Sievers, Phys. Rev. B36 (1987) 5735; T.W. Noh, P.E. Sulewski, and A.J. Sievers, Phys. Rev. B36 (1987) 8866.

[66] K.D. Cummings, J.C. Garland, and D.B. Tanner, Phys. Rev. B30 (1984) 4170.

INFRARED PROPERTIES OF THIN Pt/Al_2O_3 GRANULAR METAL-INSULATOR COMPOSITE FILMS

M. F. MacMILLAN*, R. P. DEVATY*, and J. V. MANTESE**
*University of Pittsburgh, Department of Physics and Astronomy
100 Allen Hall, Pittsburgh, PA 15260
**General Motors Research Laboratories, Electrical and Electronics
Engineering Department, Warren, MI 48090

ABSTRACT

The reflection of mid- and near-infrared radiation (400-15000 cm^{-1} by thin Pt/Al_2O_3 cermet films was measured using a Fourier transform spectrometer. The data were compared with predictions of three models for the effective optical constants of heterogeneous materials: Maxwell-Garnett, Bruggeman, and a simplified version of a probabilistic growth model due to Sheng. Sheng's model provides the best description of the data over the complete range of metallic volume fraction. This result is expected based on the most likely topology of the films and is in agreement with other work on similar systems at higher frequencies.

INTRODUCTION

The relationship between the microstructural topology, the optical properties of a heterogeneous system, and their description by an homogeneous effective dielectric function has been made clear in recent years [1]. The prediction of the optical response of a granular metal/insulator composite material over the complete range of composition provides an especially stringent challenge to effective medium theories.

In this paper, we compare the predictions of three simple effective medium models, which describe different microstructural topologies, with the measured relative reflectivity of thin Pt/Al_2O_3 films in the mid- and near-infrared. These models have been successfully applied to similar cermet systems in the near infrared and visible regions [1,2]. We find that a simplified version of a probability growth model introduced by Sheng [2,3] provides the best agreement with the data over the complete range of volume fraction. This result is not surprising since this model was developed specifically for application to cermet films. The greatest disagreement between theory and experiment occurs for metallic volume fractions near the percolation threshold for the dc conductivity. Effective medium theories are known to fail in this region[4].

EXPERIMENTAL

The Pt/Al_2O_3 granular films were prepared by coevaporation of Pt and Al_2O_3 onto single crystal sapphire wafers in a dual e-beam evaporator with a low base pressure (mid 10^{-9} torr). The volume fraction of Pt in the films, f, which ranges from 0.23 to 1.00, was determined by monitoring the relative deposition rates of the two materials using quartz crystal oscillators inside the evaporation chamber [5]. Film thicknesses, measured with a Dektak surface profilometer, ranged from 1100 to 1800 Å. The orientations of the surfaces of the sapphire substrates were determined by back reflection Laue photographs to be about 20^{o} from the ordinary axis. The percolation threshold, f_c, as determined by the temperature dependence of the dc resistivity, is in the range of 50-59% Pt by volume [6]. Although no direct determination of microstructure by electron microscopy has been performed on the films, the high value of f_c is a strong indicator of a coated-grain topology. Electron micrographs on cermet films prepared by the same method support this conclusion [7,8].

Room temperature relative reflection data were obtained using a Nicolet 740 Fourier transform infrared spectrometer with a nitrogen purge. The spectral range of 400 to 15000 cm^{-1} was covered using three combinations of sources, beamsplitters, and detectors. The resolution was 4 cm^{-1}. The samples were mounted on a Spectra Tech Model 500 variable angle specular reflectometer. The angle of incidence was 5^{o} from the normal. A 100% Pt film from the set of samples was used as the reference.

THEORY

The predictions of three effective medium theories, the Maxwell-Garnett (MG) [9], Bruggeman (BR) [10], and the Sheng probabilistic growth model (PG) [3], were compared with the data. Each model is based on a specific microstructural topology. In using these models, we assume spherical grains and homogeneity of the cermet on the scale of a wavelength.

The topology of the MG model [9] is a dielectric-coated metal sphere (one may also choose a metal-coated dielectric sphere). The thickness of the coating is determined by the metallic volume fraction of the medium, f. The effective dielectric function is

$$\epsilon_{MG} = \epsilon_o \frac{2\epsilon_o(1-f) + \epsilon_1(2f+1)}{\epsilon_o(f+2) + \epsilon_1(1-f)} \tag{1}$$

where ϵ_0 and ϵ_1 are the complex dielectric functions of the host and metal, respectively. This model is inherently asymmetric in its treatment of the constituent materials. There is no percolation transition since the metal spheres have an insulating coating for any f.

The BR model [10] treats the cermet as a collection of uncoated metal and dielectric spheres. The effective dielectric function is obtained by solving

$$\frac{3f}{2+\epsilon_1/\epsilon_{BR}} + \frac{3(1-f)}{2+\epsilon_o/\epsilon_{BR}} = 1. \tag{2}$$

This model treats the constituents in a symmetric fashion. The percolation threshold is $f_c = 1/3$.

The simplified PG model [2,3] can be regarded as a generalization of the MG model that is symmetrical in the constituent materials.
Metal-coated oxide spheres and dielectric-coated metal spheres coexist in the medium. The effective dielectric function, ϵ_{PG}, is determined by

$$\frac{3p_1}{2+\epsilon_1/\epsilon_{PG}} + \frac{3(1-p_1)}{2+\epsilon_2/\epsilon_{PG}} = 1 \tag{3}$$

where p_1 is the fraction of oxide-coated metal spheres in the composite. p_1 is related to f by means of a free volume argument by

$$p_1 = \frac{(1-f^{1/3})^3}{(1-f^{1/3})^3 + (1-(1-f)^{1/3})^3}. \tag{4}$$

ϵ_1 and ϵ_2 are the dielectric functions for the oxide-coated metal spheres and the metal-coated oxide spheres [11], respectively. This model predicts percolation at $f_c = 1/2$.

The model treats the reflection of normally incident electromagnetic radiation by a thin film on a substrate according to standard methods [12,13]. Multiple reflections within the substrate crystal were treated as incoherent. Published optical data on bulk Pt [14] and evaporated Al_2O_3 films [15] were used to calculate the optical properties of the cermet film. The substrate crystal was assumed to be aligned with the axis of symmetry normal to the surface. The oscillator parameters from Barker's fit to reflectivity data [16] were used to model the complex dielectric function of the substrate.

RESULTS AND DISCUSSION

Figure 1 compares the measured and calculated relative front reflection for three selected films. Figure 1a shows that both the MG and PG models provide good fits to the measured relative reflectivity of a f=.23 film, which has the lowest metallic volume fraction of any film in our set. The MG and PG models make similar predictions at this relatively low f because most of the coated spheres in the PG model are dielectric-coated metal spheres. The oscillatory nature of the reflectivity arises from an interference effect due to multiple reflections within the cermet film. These oscillations are less apparent in films with greater metallic composition. To obtain the fit, the thickness of the film was assumed to be 2200 Å, whereas the measured value was 1525 Å. The structure below 1500 cm^{-1} is due to optic phonons in the Al_2O_3 host and substrate.

Figure 1b shows the results for a film with f=.58. This volume fraction is near the percolation threshold for this system [6]. The measured film thickness of 1475 Å was used in the calculations. None of the models describes the data very well. This result is in agreement with recent work showing that effective medium theories do not apply near percolation [4]. Details of cluster morphology not included in the effective medium treatment, such as nonspherical shape, are most important near f_c. The rather flat frequency dependence of the relative reflectivity is also a characteristic feature near f_c [4,17]. The MG model best fits the magnitude of relative reflectivity, but the BR and PG models provide a better description of the frequency dependence.

Figure 1c shows that the BR and PG models provide the best fits to a 1300 Å thick film with f=.83. The agreement with the MG model is poor. A reverse MG model using metal-coated dielectric spheres would provide a better description. In fact, this is the dominant topology of the PG model for f near unity.

Berthier and Lafait [18] have studied the infrared properties of Pt/Al_2O_3 cermet films prepared by rf cosputtering. They were able to fit the measured optical constants using the BR model over a broad range of composition. However, they treated the volume fraction as an adjustable parameter and introduced an effective depolarization factor as well. The BR model, with fewer adjustable parameters, does not apply to our films, which were prepared by a different method.

In conclusion, we find that the PG model provides the best description, among three simple effective medium theories, of the relative reflectivity of thin Pt/Al_2O_3 granular cermet films over the complete range of composition, although the agreement is not quantitative, particularly near f_c. We intend to extend this work by measuring the absolute reflectivity using the W-V method and to extract the frequency dependent complex index of refraction of films for which the transmission is also measurable.

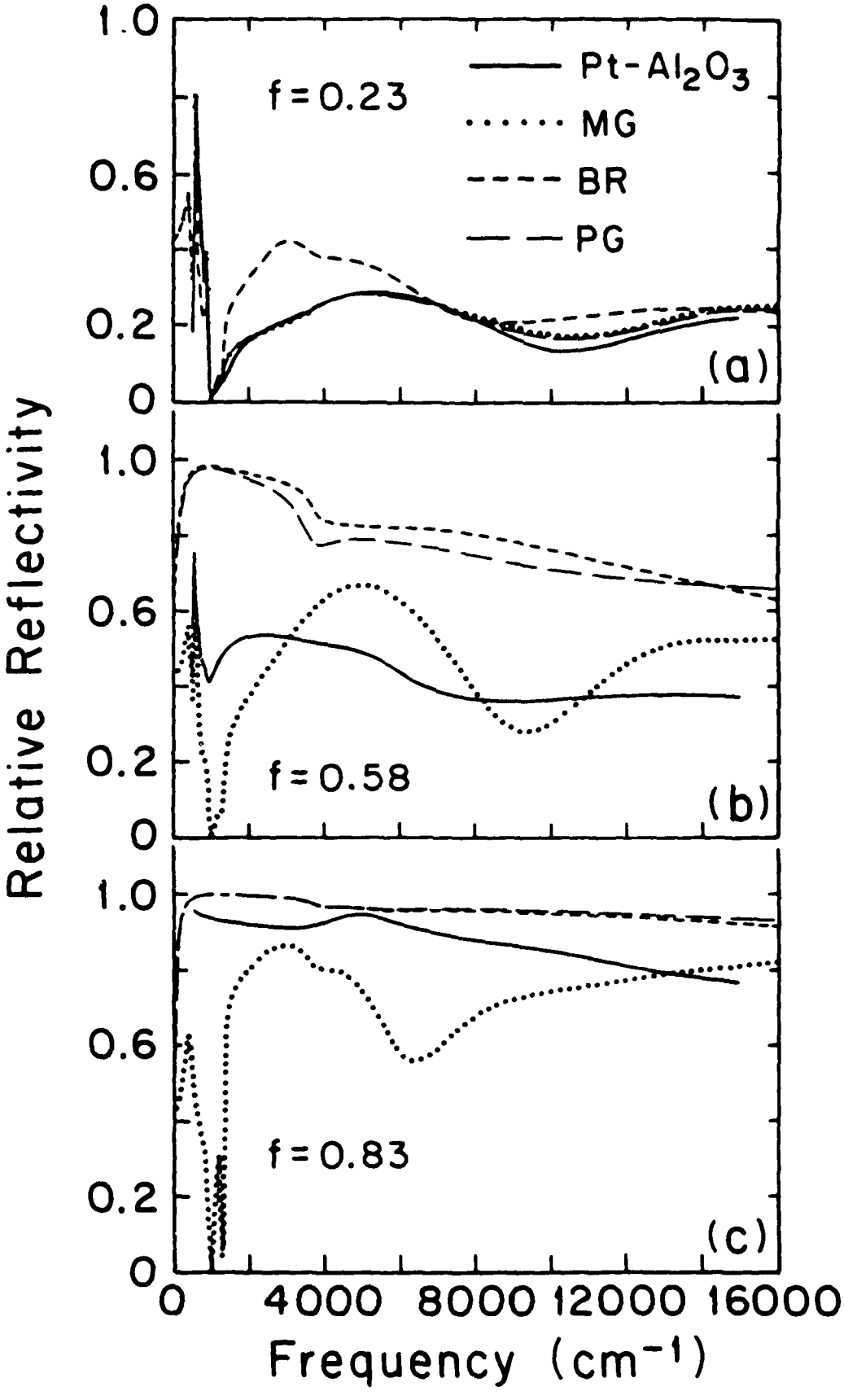

Figure 1: Composition dependence of relative front reflectivity of Pt/Al_2O_3 granular composite films. A Pt film is the reference. The predictions of the three models discussed in the text are also shown.

ACKNOWLEDGEMENT

This work was supported by ONR Contract #N00014-85-K-0808.

REFERENCES

[1] U. J. Gibson, H. G. Craighead, and R. A. Buhrman, Phys. Rev. B25, 1449 (1982).

[2] U. J. Gibson and R. A. Buhrman, Phys. Rev. B27, 5046 (1983).

[3] Ping Sheng, Phys. Rev. Lett. 45, 60 (1980).

[4] Y. Yagil and G. Deutscher, Appl. Phys. Lett. 52, 374 (1988), and references therein.

[5] J. V. Mantese, Ph.D. Thesis, Cornell University, 1985.

[6] J. V. Mantese, W. A. Curtin, and W. W. Webb, Phys. Rev. B33, 7897 (1986).

[7] H. G. Craighead, Ph.D. Thesis, Cornell University, 1980.

[8] U. J. Gibson, Ph.D. Thesis, Cornell University, 1982.

[9] J. C. M. Garnett, Phil. Trans. R. Soc. London, Ser A203, 385 (1904).

[10] D. A. G. Bruggeman, Ann. Phys. (Leipzig) 24, 636 (1936).

[11] H. C. van der Hulst, Light Scattering by Small Particles (Wiley, New York, 1957).

[12] Z. Knittl, Optics of Thin Films (Wiley, New York, 1976).

[13] O. S. Heavens, Optical Properties of Thin Solid Films (Butterworths Publications, Ltd., London, 1955).

[14] D. W. Lynch and W. R. Hunter, in Handbook of Optical Constants of Solids, edited by E. Palik (Academic Press, New York, 1985).

[15] T. S. Eriksson, A. Hjortsberg, G. A. Niklasson, and C. G. Granqvist, Appl. Opt. 20, 2742 (1981).

[16] A. S. Barker, Jr., Phys. Rev. 132, 1474 (1963).

[17] P. Gadenne, A. Beghdadi, and J. Lafait, Optics Commun. 65, 17 (1988).

[18] S. Berthier and J. Lafait, J. Physique 47, 249 (1986).